

# Examination of the role of detritus food quality, phytoplankton intracellular storage capacity, and zooplankton stoichiometry on planktonic dynamics

Gurbir Perhar, George B. Arhonditsis\*

Ecological Modeling Laboratory, Department of Physical and Environmental Sciences, University of Toronto, Toronto, Ontario, Canada, M1C 1A4

## ARTICLE INFO

### Article history:

Received 20 February 2012

Received in revised form 13 June 2012

Accepted 14 June 2012

Available online 21 June 2012

### Keywords:

Intracellular nutrient storage

Seston food quality

Stoichiometric theory

Highly unsaturated fatty acids

Plankton dynamics

## ABSTRACT

Nutrient stoichiometric ratios are primary driving factors of planktonic food web dynamics. Ecological stoichiometry theory postulates the elemental ratios of consumer species to be homeostatic, while primary-producer stoichiometry may vary with ambient nutrient availability. The notion of phytoplankton intracellular storage is far from novel, but remains largely unexplored in modeling studies of population dynamics. We constructed a seasonally-unforced, zero-dimensional, nutrient–phytoplankton–zooplankton–detritus (NPZD) model that considers dynamic phytoplankton phosphorus reserves and quasi-dynamic zooplankton stoichiometry. A generic food quality term is used to express seston biochemical composition, ingestibility, and digestibility. We examined the sensitivity of the planktonic food web patterns to light and nutrient availability, zooplankton mortality, and detritus food quality as well as to phytoplankton intracellular storage and zooplankton stoichiometry. Our results reinforce earlier findings that high quality seston exerts a stabilizing effect on food web dynamics. However, we also found that the combination of low algal and high detritus food quality with high zooplankton mortality yielded limit cycles and multiple steady states, suggesting that the heterogeneity characterizing seston nutritional quality may have more complicated ecological ramifications. Our numerical experiments identify resource competition strategies related to nutrient transport rates and internal nutrient quotas that may be beneficial for phytoplankton to persevere in resource-limiting habitats. We also highlight the importance of the interplay between optimal stoichiometry and the factors controlling homeostatic rigidity in zooplankton. In particular, our predictions show that the predominance of phosphorus-rich and tightly-homeostatic herbivores in nutrient-enriched environments with low seston food quality can potentially result in high phytoplankton abundance, high phytoplankton-to-zooplankton ratios, and acceleration of oscillatory dynamics. Generally, our modeling study emphasizes the impact of both intracellular/somatic storage and food quality on prey–predator interactions, pinpointing an important aspect of food web dynamics usually neglected by the contemporary modeling studies.

© 2012 Elsevier B.V. All rights reserved.

## 1. Introduction

Stoichiometrically explicit models acknowledge the constraints imposed by mass balance of multiple elements during ecological interactions (Elser and Urabe, 1999). In the case of freshwater zooplankton, experimental evidence suggests a relationship linking maximal growth rates to somatic phosphorus content through ribosomal RNA and protein synthesis (DeMott and Pape, 2005). The content of recycled material within a system appears to be a function of producer and consumer stoichiometries, in addition to the consumer's ability to sequester growth limiting nutrients (Sterner, 1990). Elser and Urabe (1999) asserted that many contemporary studies overlook the importance of zooplankton nutrient recycling as a regulatory factor of the lower food web dynamics. Resource ratio competition theory postulates the mismatch between somatic ratios of producers and consumers to be the primary driving force

behind consumer-driven nutrient recycling (Elser and Urabe, 1999; Lehman, 1984). Structural shifts in planktonic communities may be a result of these observations, as existing evidence suggests that phytoplankton tends to be phosphorus-limited in ecosystems dominated by P-rich daphnids, whereas copepod-dominated systems are characterized by nitrogen-limited phytoplankton (Elser et al., 1988). Additional consequences of nutrient limitation include possible morphological changes in nutrient stressed algae, such as increasing thickness and lignin content of the cell wall (Ravet and Brett, 2006; Van Donk and Hesson, 1993). This adaptive strategy may reduce the algal palatability and digestibility to zooplankton, i.e., the so-called indirect nutrient limitation (Ravet and Brett, 2006).

Many empirical studies have examined the impact of seston biochemical food quality on zooplankton somatic growth (Guisande et al., 2000; Müller-Navarra, 1995). Guisande et al. (2000) reported the importance of seston food quality to the reproductive success of the copepod *Euterpina acutifrons*. They measured both food quantity based on protein availability in the food, and quality based on the disparity among

\* Corresponding author. Tel.: +1 416 208 4858; fax: +1 416 287 7279.  
E-mail address: [georgea@utsc.utoronto.ca](mailto:georgea@utsc.utoronto.ca) (G.B. Arhonditsis).

somatic, egg and seston amino acid composition. Food quantity was the main driving factor in egg production, but egg hatching success was highest when amino acid composition was most similar across somatic tissue, seston and eggs (Guisande et al., 2000). Müller-Navarra (1995) studied growth rates for the freshwater cladoceran *Daphnia galeata*, based on elemental (carbon, nitrogen, phosphorus) and biochemical (fatty acids) seston content. *Daphnia* growth was characterized by a very weak causal association with seston phosphorus, a significantly stronger link with both nitrogen and carbon, and an exceptionally strong dependence upon eicosapentaenoic acid (20:5 n3) availability; a highly unsaturated fatty acid (HUFA; Müller-Navarra, 1995). Fatty acids are hydrocarbon chains of differing lengths and bonding patterns with very important role in planktonic food webs. Most animals are unable to synthesize longer chain fatty acids (HUFAs), and must acquire these potentially growth limiting compounds through diet, i.e., HUFA-rich algal groups (diatoms, cryptophytes). Yet, although a great deal of research has shed light on the role of HUFAs at the individual animal level, e.g., zooplankton allocation of essential lipids during exposure to poor food quality (Wacker and Martin-Creuzburg, 2007), lipid allocation during reproduction (Smyntek et al., 2008), and internal HUFA reserves relative to diet (Brett et al., 2006), the ramifications of HUFA limitation in the context of plankton population dynamics have not been adequately examined as of yet.

Significant work has also been done towards the elucidation of the causal link between phytoplankton biochemical content and zooplankton assimilation/growth (DeMott and Müller-Navarra, 1997; Brett et al., 2000; 2006). Data from these studies can be incorporated into theoretical mathematical models, giving researchers the ability to place individual observations in the context of population dynamics. From a bottom-up perspective, consumer biomass is generally considered to be controlled by food abundance, but systems of high energy coupled with producers of low nutritional value fail to fit this pattern (Loladze et al., 2000). Balancing food quantity with quality is an integral part of accurately capturing trophic energy transfers. Recently, a group of modeling studies began incorporating food quality into plankton population models as a combined index of food ingestibility, digestibility, and biochemical content (Arhonditsis and Brett, 2005a,b; Danielsdottir et al., 2007; Perhar and Arhonditsis, 2009). The predicted plankton patterns suggest that both algal (Arhonditsis and Brett, 2005b; Danielsdottir et al., 2007), and detrital (Perhar and Arhonditsis, 2009) food quality can profoundly affect aquatic food webs and energy transfer among trophic levels. In particular, Perhar and Arhonditsis (2009) reported food webs with high quality primary producers at the base can sustain zooplankton in high abundance, suppressing phytoplankton biomass to low levels. Low quality algae resulted in weak trophic cascades and led to predominance of the bottom-up control, whereby primary production was only determined by nutrients and light availability. Moreover, the inclusion of a detritus compartment pinpointed the importance of an alternate food source in planktonic systems. Specifically, the decline of algal food quality in response to nutrient enrichment renders a predominant role to detritus quality, which in turn appears to modulate system stability and resilience (Perhar and Arhonditsis, 2009). While algal stoichiometries have long been accepted as being dynamic, the vast majority of the contemporary modeling studies fail to account for dynamic consumer stoichiometries (Mulder and Bowden, 2007). There is also an important gap in the modeling literature in regards to the effects of intracellular nutrient storage on plankton population dynamics, while taking into consideration both stoichiometric and biochemical food quality limitations.

In this study, our objective is to incorporate dynamic producer and grazer stoichiometries into the existing four compartment nutrient-phytoplankton-zooplankton-detritus (NPZD) population model introduced by Perhar and Arhonditsis (2009). Our goal is to examine the capacity of cellular and somatic nutrient strategies to shape population level dynamics. As such, parameters controlling intracellular storage such as minimum and maximum phytoplankton phosphorus quota (Droop, 1968), and maximum phosphorus uptake rate, as well as

parameters controlling zooplankton stoichiometry will be thoroughly investigated. Additional experiments testing top-down and bottom-up controls exerted by light and nutrient availability, zooplankton mortality and detritus food quality will be conducted, drawing direct parallels to Perhar and Arhonditsis' (2009) study. We will carry out phase space explorations and bifurcation analysis to ascertain the role of the different stoichiometric and intracellular nutrient storage parameters. Building upon our earlier work, the consideration of dynamic stoichiometry and intracellular storage is a natural progression for further elucidating the interactions taking place at the producer-consumer interface.

## 2. Methods

### 2.1. Model description

We use a zero-dimensional and seasonally-unforced model that aims to reproduce plankton dynamics in a well-mixed epilimnetic environment. Using contemporary advances in ecological stoichiometry, we explicitly account for the interplay between ambient nutrient concentrations and plankton intracellular/somatic storage. By doing so, we aim to explore the ecological implications of dynamic primary producer cellular and consumer somatic stoichiometries. Our model builds upon the mathematical framework of the Perhar and Arhonditsis (2009) theoretical study, with four compartments (phosphate, phytoplankton, zooplankton, detritus), and added consideration for dynamic primary producer and grazer stoichiometries (Table 1). The phosphate equation considers uptake by phytoplankton and the portion of zooplankton mortality/higher predation that is recycled into the system as dissolved-phase phosphorus. Epilimnetic phosphate levels are fuelled by the detritus mineralization, and are also modulated by the diffusive mixing with the hypolimnion. The detritus pool is expressed in units of both carbon ( $DET_C$ ) and phosphorus ( $DET_P$ ). Detritus sinks out of the epilimnion at a constant rate and is transformed to phosphate by the mineralization processes. Phytoplankton respiration and a fraction of the zooplankton growth that represents the fecal pellets/egested material also contribute to the detritus stock.

The phytoplankton equation considers production and losses due to basal metabolism, settling and herbivorous zooplankton grazing. The phytoplankton internal pool of phosphorus is replenished by nutrient uptake, following Michaelis-Menten kinetics, while a feedback term ensures rapid or slow uptake when the internal reserves are low or high, respectively (Zhao et al., 2008a). Utilization of the internal phosphorus pool is associated with the demands for algal growth. Light availability is another factor that determines phytoplankton biomass production and light extinction in the water column stems from background light attenuation and the algal self-shading effects. Phytoplankton sinks out of the mixed layer at a constant rate.

Zooplankton grazing and losses due to natural mortality/consumption by higher predators are the two main terms in the zooplankton biomass equation. Zooplankton has two available food sources (phytoplankton and detritus) of equal palatability ( $\omega = 1$ ). A fraction of zooplankton grazing is assimilated and fuels growth; both herbivory and detritivory were formulated using the Holling Type III function. Phosphorus assimilation efficiency is directly related to the "food quality" concentration ( $FQ$ ), a variable that encompasses the effects of both food quantity and quality, on the energy flow across food webs (Arhonditsis and Brett, 2005a). Food quality is dynamically characterized on the basis of two factors: i) the imbalance between the C:P ratio of the grazed seston and a critical  $C:P_{OzooP}$  ratio above which zooplankton growth is limited by P availability; and ii) the variability in food quality due to differences in highly unsaturated fatty acid, amino acid, protein content and/or digestibility. A hyperbolic formula is employed to relate phosphorus assimilation efficiency with the "food quality" concentration. Zooplankton somatic P:C is modeled explicitly to quantify its disparity from optimal stoichiometry, making use of Mulder and Bowden's (2007) "regulatory coefficient". Namely, optimal and minimum somatic phosphorus values

**Table 1**  
Specific functional forms of the plankton model.

$\frac{dPO_4}{dt} = -P_{UP}P_{FB}PHYT + \gamma d \frac{ZOO P^3}{pred^2 + ZOO P^2} P/C_{ZOO P} + \phi DET_P + k(PO_{4(hypo)} - PO_4)$	
$\frac{dPHYT}{dt} = f(P) \frac{a}{b+cPHYT} PHYT - rPHYT - \frac{NPHYT^2}{\mu^2 + PHYT^2 + \omega DET_C^2} ZOO P - (s+k)PHYT$	
$\frac{dP_{INT}}{dt} = P_{UP}P_{FB} - growthP_{INT}$	
$\frac{dZOO P}{dt} = \frac{a_c \lambda (PHYT^2 + \omega DET_C^2)}{\mu^2 + PHYT^2 + \omega DET_C^2} ZOO P - d \frac{ZOO P^3}{pred^2 + ZOO P^2}$	
$\frac{dDET_C}{dt} = rPHYT + \frac{[PHYT^2 - \alpha_P C/P_{ZOO P} (PHYT^2 P_{INT} - \omega DET_C DET_P)] \lambda}{\mu^2 + PHYT^2 + \omega DET_C^2} ZOO P - (k + \varphi + \psi) DET_C$	
$\frac{dDET_P}{dt} = rPHYT P_{INT} + \frac{[(1 - \alpha_P) PHYT^2 P_{INT} - \alpha_P \omega DET_C DET_P] \lambda}{\mu^2 + PHYT^2 + \omega DET_C^2} ZOO P - (k + \varphi + \psi) DET_P$	
$\alpha_C = \frac{C/P_{ZOO P} \alpha_P (PHYT^2 P_{INT} + \omega DET_C DET_P)}{PHYT^2 + \omega DET_C^2}$	$\alpha_P = \frac{\alpha_{P1} FQ}{\alpha_{P2} + FQ}$
$FQ = (FQ_1^2 \sqrt{PHYT} + FQ_2^2 \sqrt{DET_C}) ZOO P_{C/PLIM}$	
$ZOO P_{C/PLIM} = \begin{cases} 1 & \text{if } Graz_{C/P} \leq C/P_{OZOO P} \\ \frac{C/P_{OZOO P}}{Graz_{C/P}} & \text{if } Graz_{C/P} > C/P_{OZOO P} \end{cases}$	$Graz_{C/P} = \frac{(PHYT^2 + \omega DET_C^2)}{(PHYT^2 P_{INT} + \omega DET_C DET_P)}$
$P_{UP} = P_{UPMAX} \frac{PO_4}{K_P + PO_4}$	$growth = f(P) \frac{a}{b+cPHYT}$
$P_{FB} = \frac{P_{MAX} - P_{INT}}{P_{MAX} - P_{MIN}}$	$f(P) = \frac{P_{INT} - P_{MIN}}{P_{MAX} - P_{MIN}}$
$P/C_{ZOO P} = P/C_{OZOO P} - \left(1 - \frac{P_i}{P/C_{OZOO P}}\right)^N (P/C_{OZOO P} - P/C_{MZOO P})$	$P_i = \frac{P_{INT} PHYT + DET_P}{PHYT + DET_C}$

are parameterized and play a significant role in determining the variability of zooplankton somatic  $P:C$ , as does the regulatory coefficient in modulating the impact of the discrepancy between seston stoichiometry and zooplankton optimal  $P:C$  ratio. Finally, a sigmoidal closure term was selected to represent a “switchable”-type of predator behavior controlled by a threshold prey concentration (Edwards and Yool, 2000).

## 2.2. Modeling experiments

A series of phase space explorations were designed to test the sensitivity of certain ecological factors, such as detritus food quality ( $FQ_2$ ), hypolimnetic nutrient concentration ( $PO_{4(hypo)}$ ), light attenuation ( $b$ ) and zooplankton mortality ( $d$ ). System dynamics induced by parameter variations were tracked through phytoplankton biomass levels and regions of steady state vs. limit cycle behavior. Presence of a steady-state equilibrium (i.e., steady biomass with no oscillations) is indicative of a robust system; one which can withstand potential ecological perturbations, i.e., invasive species, episodic meteorological events and associated nutrient pulses. Manifestation of oscillatory behavior and possible multiple steady states implies vulnerability to the aforementioned disturbances, and therefore susceptibility to abrupt changes in ecosystem state. Each experiment tested one parameter against another in a continuous manner, while discretely varying the third and holding the fourth constant. Similar to Perhar and Arhonditsis (2009), scenarios were created thematically, i.e., nutrient vs. energy enrichment, top-down vs. bottom-up control, and the interplay between detritus food quality and zooplankton mortality. Using MatCont, a continuation toolbox in Matlab (Dhooge et al., 2003), we also conducted bifurcation analysis to gauge system response to varying detritus food quality. Another set of phase space explorations was designed to test the impact of the six parameters, controlling phytoplankton intracellular storage capacity and zooplankton stoichiometry (see Table 2 for complete list of parameters). Throughout all of the experiments, the phytoplankton parameterization was held constant, representing a K-strategist with low maximum growth and metabolic rates, slow  $P$  kinetics, high tolerance to low light availability, low settling velocity, and low food quality. This characterization resembles a cyanobacteria-dominated phytoplankton community and was found to increase the susceptibility of planktonic food webs to the interplay between bottom-up and top-down forces as well as to accelerate the manifestation of oscillatory patterns (Perhar and Arhonditsis, 2009).

## 3. Results

### 3.1. What is the interplay between bottom-up regulatory factors at the producer–grazer interface?

The availability of energy and nutrients at the plant–animal interface can significantly shape the dynamics taking place in the lower food web. To gain insights into the interplay between these two ecological factors as postulated by our model structure, we ran simulations explicitly examining light attenuation against hypolimnetic nutrient levels at three different zooplankton mortality values while the detritus food quality was set at low levels. Hypolimnetic nutrients can potentially represent a nutrient recharge source in the epilimnion, and can be thought of as a surrogate of nutrient availability to phytoplankton. Under low zooplankton mortality/fish predation conditions, phytoplankton biomass was very low in the region of high light attenuation (i.e., low light availability) and low nutrient levels (Fig. 1a). The ratio of phytoplankton to zooplankton biomass in the same region was consistently greater than one, indicating an even lower zooplankton standing biomass (Fig. 1b). The region experiencing unforced oscillations is bound by a white contour line and is localized to areas of high energy and nutrient availability. Notably, the phytoplankton:zooplankton ratio often falls below one in this unstable region, while the plankton dynamics frequently follow a boom-bust pattern rather than a smooth sinusoidal trajectory (see Figs. 1 and 2 in the Electronic Supplementary Material). Increasing zooplankton mortality yielded larger phytoplankton biomass values along with a wider oscillatory region (Fig. 1c) and extremely low zooplankton biomass relative to phytoplankton (Fig. 1d). Further increase of the zooplankton mortality resulted in very high phytoplankton biomass (Fig. 1e), negligible zooplankton biomass relative to phytoplankton (Fig. 1f), and an extremely unstable system with unforced oscillations present throughout the range scanned. In this set of experiments, the lack of strong zooplankton presence in the regions explored partly stems from the poor food quality of phytoplankton and detritus, which effectively promotes a decoupling at the producer–grazer interface. Finally, aside from the scenario of high zooplankton mortality, we note that the mathematical formulations adopted result in approximately orthogonal effects of the nutrient and light availability on the planktonic patterns, whereby  $PO_{4(hypo)} < 0.04 \text{ g P m}^{-3}$  approximately sets the boundary of the phosphorus limiting zone.

**Table 2**  
Parameter definitions of the plankton model.

Variable	Symbol	Initial	Units		
Phosphate	$PO_4$	0.5	$g P m^{-3}$		
Phytoplankton biomass	$PHYT$	0.1	$g C m^{-3}$		
Phytoplankton internal phosphorus	$P_{INT}$	0.0165	$g P (g C)^{-1}$		
Zooplankton biomass	$ZOOP$	0.05	$g C m^{-3}$		
Detritus carbon	$DET_C$	0.08	$g C m^{-3}$		
Detritus phosphorus	$DET_P$	0.01	$g P m^{-3}$		
Parameter	Symbol	Default	Units		
Maximum phytoplankton growth rate	$a$	0.1	$m^{-1} day^{-1}$		
Phytoplankton self-shading coefficient	$c$	0.05	$m^2 (g C)^{-1}$		
Half-saturation constant for predation	$pred$	0.03	$g C m^{-3}$		
Half-saturation constant for $PO_4$ uptake	$K_p$	0.03	$g P m^{-3}$		
Cross-thermocline exchange rate	$k$	0.05	$Day^{-1}$		
Phytoplankton respiration rate	$r$	0.05	$Day^{-1}$		
Phytoplankton sinking loss rate	$s$	0.001	$Day^{-1}$		
Zooplankton growth efficiency for phosphorus	$\alpha_{p1}$	0.9	Dimensionless		
Half saturation constant for zooplankton growth efficiency	$\alpha_{p2}$	0.03	$(g C m^{-3})^{-1/2}$		
Phytoplankton food quality	$FQ_1$	0.2	Dimensionless		
Regeneration of zooplankton predation excretion	$\gamma$	0.6	Dimensionless		
Maximum zooplankton grazing rate	$\lambda$	0.6	$Day^{-1}$		
Zooplankton grazing half-saturation constant	$\mu$	0.035	$g C m^{-3}$		
Relative zooplankton preference for detritus	$\omega$	1	Dimensionless		
Detritus remineralization rate	$\varphi$	0.17	$Day^{-1}$		
Detritus sinking rate	$\psi$	0.3	$Day^{-1}$		
Maximum phytoplankton internal phosphorus	$P_{MAX}$	0.0285	$g P (g C)^{-1}$		
Minimum phytoplankton internal phosphorus	$P_{MIN}$	0.009	$g P (g C)^{-1}$		
Maximum phosphorus uptake rate	$P_{UPMAX}$	0.01	$g P (g C)^{-1} day^{-1}$		
Optimal phosphorus to carbon ratio for zooplankton	$P/C_{zoop}$	0.024	$g P (g C)^{-1}$		
Minimum phosphorus to carbon ratio for zooplankton	$P/C_{mzoop}$	0.004	$g P (g C)^{-1}$		
Regulatory coefficient	$N$	2	Dimensionless		
Parameter	Symbol	Low	Int.	High	Units
Background light attenuation	$b$	0.05	0.10	0.15	$m^{-1}$
Higher predation on zooplankton	$d$	0.1	0.25	0.4	$Day^{-1}$
Hypolimnetic phosphate concentration	$PO_4(hypo)$	0.03		1	$g P m^{-3}$
Detritus food quality	$FQ_2$	0.2	0.5	0.8	Dimensionless

### 3.2. To what extent is the bottom-up control at the producer–grazer interface confounded by the impact of top-down control?

The previous experiment provides evidence of a substantial interplay between bottom-up control and zooplankton mortality. To test the combined influence of top-down and bottom-up control, zooplankton mortality and light attenuation were scanned in a continuous manner at three levels of detritus food quality, while the likelihood of nutrient limitation was eliminated by assigning a high value to the hypolimnetic nutrient concentration. When using low detritus food quality, the diagonal patterns of change of the phytoplankton biomass as well as the delineated oscillatory region are indicative of covariance of the two factors examined at moderate zooplankton mortality values (Fig. 2a). Yet, extreme zooplankton mortality levels (both high and low) yielded either very high or very low phytoplankton biomass with limited influence of the light availability. Throughout the region scanned, zooplankton biomass was very low relative to phytoplankton, with the largest phytoplankton to zooplankton biomass ratios located in regions of high light attenuation and high zooplankton mortality, i.e., extreme bottom-up stress combined with extreme top-down stress (Fig. 2b). Increasing the nutritional quality

of detritus shifted the oscillatory region at higher zooplankton mortality levels and narrowed down the light attenuation levels under which unforced oscillations occur (Fig. 2c,e). Further, the increase of detritus food quality gradually yielded lower phytoplankton biomass levels and lower phytoplankton to zooplankton ratios (Fig. 2d,f). The importance of detritus as an alternative food source lies in its ability to offset food shortages for zooplankton, which can subsequently withstand greater mortality levels and may exert stronger control on the phytoplankton standing biomass. Interestingly, a conceptually similar experiment that considers the nutrient (instead of light) availability as a surrogate of the bottom-up control supports similar conclusions regarding the role of detritus food quality (Fig. 3 in the Electronic Supplementary Material). We also note that both the patterns of change of the phytoplankton biomass and the shape of the oscillatory regions suggest orthogonality (rather than covariance) on the impact of the limiting nutrient and zooplankton mortality.

### 3.3. What is the role of an alternate food source in a system with primary producers of poor nutritional quality?

Hitherto, our findings pinpoint the regulatory role of a reliable alternate food source for zooplankton, and the next experiment more rigorously tests the influence of detritus food quality with zooplankton mortality on the producer–grazer interface. Three levels of the light availability were considered and the hypolimnetic nutrient concentration was set high to minimize the likelihood of nutrient limitation. When low light availability is assumed, phytoplankton once again peaks in regions of high zooplankton mortality ( $d > 0.12$ ), although its response covaries with the detritus food quality (Fig. 3a). With the exception of extremely high zooplankton mortality combined with extremely low detritus food quality (i.e., highly stressed grazers), the same conditions give rise to unforced oscillations, whereas steady states typically characterize the areas of high detritus food quality and/or low zooplankton mortality. Notably, this subregion of the parameter space examined yields low phytoplankton abundance, as the higher detritus food quality sustains zooplankton at levels that are unable to attain by exclusively feeding upon poor quality algae. Consequently, the reduced top down stress may permit zooplankton to suppress phytoplankton, albeit with primary producers still outnumbering grazers at a ratio of approximately 2:1 (Fig. 3b). Finally, the gradual reduction of the light attenuation broadens the oscillatory regions, but these instability patterns are not accompanied by notable changes of the phytoplankton biomass and the phytoplankton to zooplankton ratios (Fig. 3c–f).

Bifurcation analysis offers another means to gain insights into the effects of incremental changes in detritus food quality on plankton dynamics. Under conditions of low zooplankton mortality and high light availability, the equilibrium trajectory depicts the stability patterns stemming from the high detritus food quality (Fig. 4a). Yet, the planktonic system experiences a sub-critical Neimark–Sacker point<sup>1</sup> with the gradual lowering of the detritus food quality, thereby entering an area where unforced oscillations occur, as represented by the cloud of points around the unsteady equilibrium trajectory. Lowering light availability while maintaining low levels of zooplankton mortality eliminates all unforced oscillations (the first dashed line shown in Fig. 3a), resulting in a steady state equilibrium throughout the range scanned (Fig. 4b). Increasing zooplankton mortality with high light availability produced a larger region of instability (Fig. 4c), requiring very high detritus food quality to bring the system back to equilibrium. The same zooplankton mortality level combined with low light availability yielded a much more stable system and somewhat smaller oscillation amplitudes (e.g., see the range of the plankton biomass axes in Fig. 4d). A

<sup>1</sup> Bifurcation resulting in the appearance of an invariant torus near a periodic orbit. [See also Fig. 4 in Electronic Supplementary Material.]



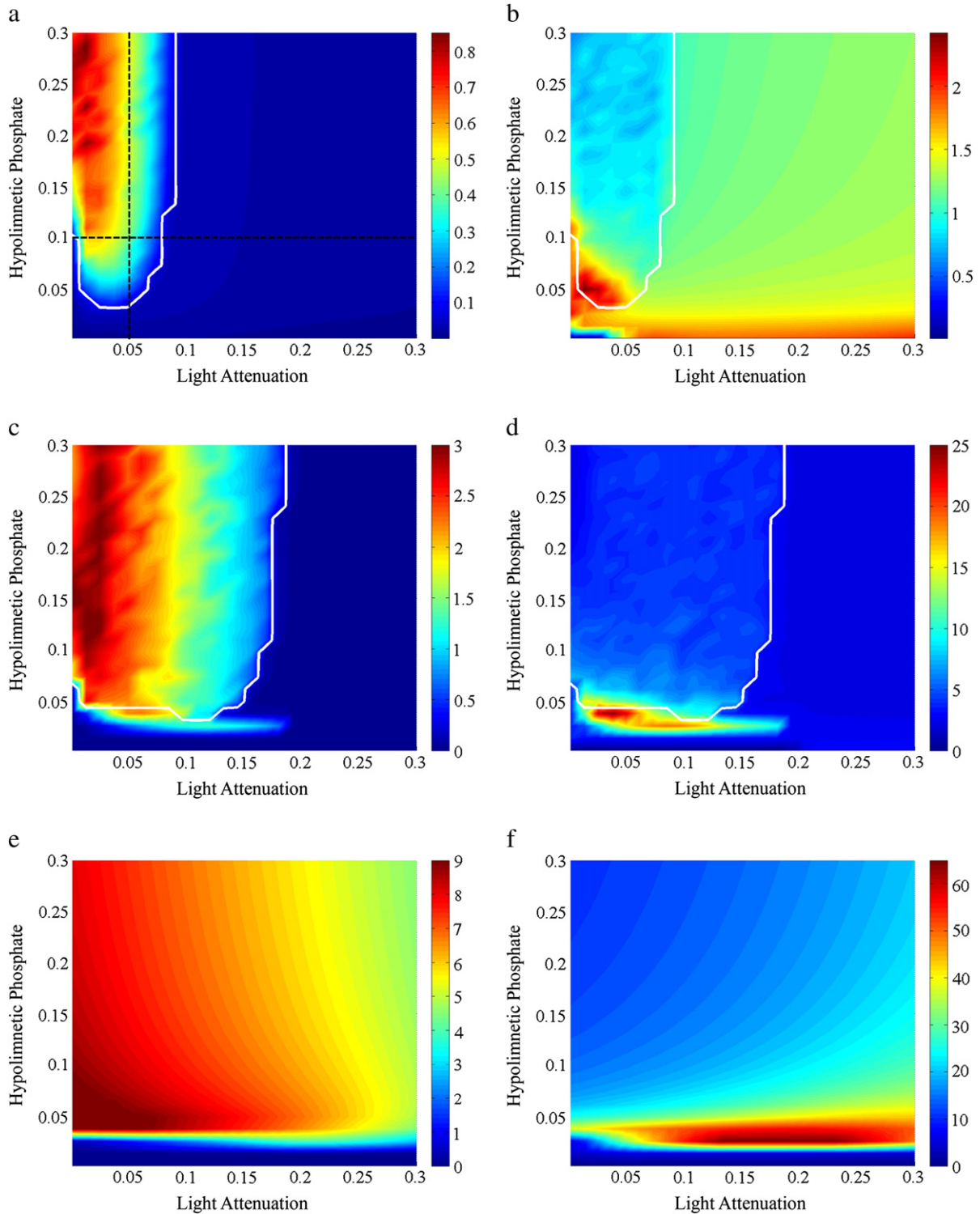


**Fig. 1.** Parameter space exploration between parameters controlling light ( $b$ ) and nutrient availability ( $PO4_{(hypo)}$ ). The color map depicts phytoplankton biomass in panels a,c,e and phytoplankton to zooplankton ratio in panels b,d,f; the white contour delineates the oscillatory region(s). Detritus food quality is set low ( $FQ_2 = 0.2$ ), while zooplankton mortality ranges from low (panels a and b,  $d = 0.1 \text{ day}^{-1}$ ), to intermediate (panels c and d,  $d = 0.25 \text{ day}^{-1}$ ), and to high (panels e and f,  $d = 0.4 \text{ day}^{-1}$ ) values. Black dashed lines represent trajectories scanned in Figs. 1 and 2 of the Electronic Supplementary Material.

Hopf bifurcation point<sup>2</sup> with a nearby limit point of cycles (Fig. 4d insert) is indicative of a subcritical bifurcation,<sup>3</sup> whereby the system

<sup>2</sup> Local bifurcation in which a fixed point of a dynamical system loses stability as a pair of complex conjugate eigenvalues of the linearization around the fixed point crosses the imaginary axis of the complex plane. Results in the appearance of a small amplitude periodic orbit. [See also Fig. 4 in Electronic Supplementary Material.]

<sup>3</sup> Bifurcation in which limit cycle orbit is unstable.

folds backward to achieve stable orbits. The latter pattern was observed throughout our bifurcation analyses. Further increase in zooplankton mortality dramatically alters the plankton dynamics (Fig. 4e). Whereas earlier, interface stability was resultant of high quality detritus, high zooplankton mortality combined with high food quality yielded unforced oscillations. Extremely high zooplankton mortality may be releasing phytoplankton from herbivorous grazing (very large phytoplankton

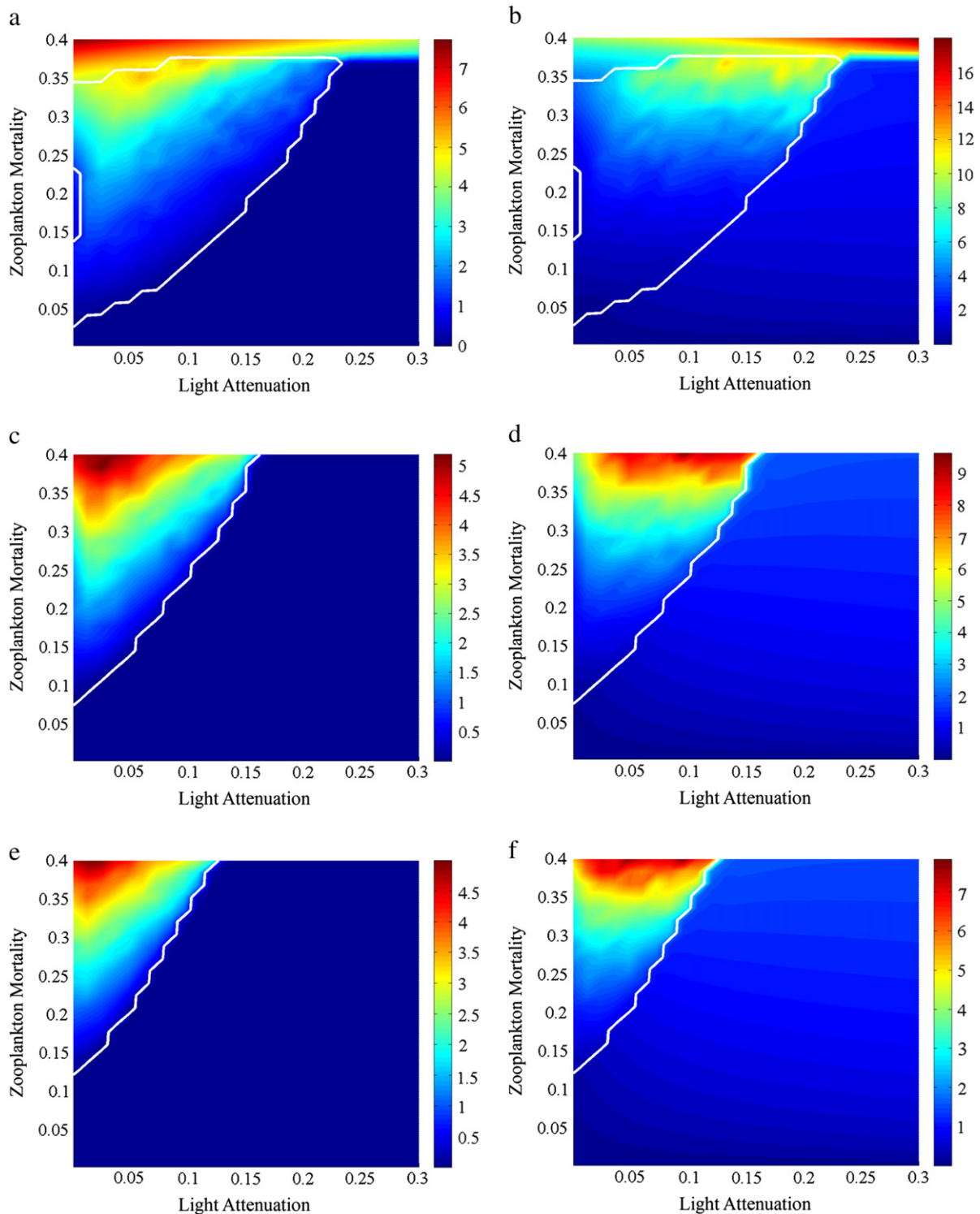


**Fig. 2.** Parameter space exploration testing bottom-up vs. top-down control via parameters regulating light (*b*) and zooplankton mortality (*d*). The color map depicts phytoplankton biomass in panels a,c,e and phytoplankton to zooplankton ratio in panels b,d,f; the white contour delineates the oscillatory region(s). Hypolimnetic nutrient concentration is set high ( $PO4_{(hypo)} = 1 \text{ g P m}^{-3}$ ), while detritus food quality is varied from low (panels a and b,  $FQ_2 = 0.2$ ), to intermediate (panels c and d,  $FQ_2 = 0.5$ ), and to high (panels e and f,  $FQ_2 = 0.8$ ) values.

biomass combined with relatively low zooplankton biomass in Fig. 4e), but the presence of a reliable alternate food source (high detritus food quality) may allow zooplankton to persevere and avoid elimination from the system. Lowering light availability with increased zooplankton mortality once again produced a stable interface with low zooplankton biomass when detritus food quality is low. However, the unforced oscillations with increasing food quality ended abruptly and the interface settled to another steady state where

both the producer and grazer have low biomass levels. The sudden shift from oscillations to a steady state, e.g., when detritus food quality equals to 0.55 in Fig. 5a, was caused by the collision of an unstable state (dashed line) with a steady state attractor resulting in a global bifurcation. In essence, the system short-circuited itself: when an unstable attractor makes contact with a steady state attractor, the plant-animal interface jumps from one to the other. With this short circuiting, the points of interest (i.e., neutral

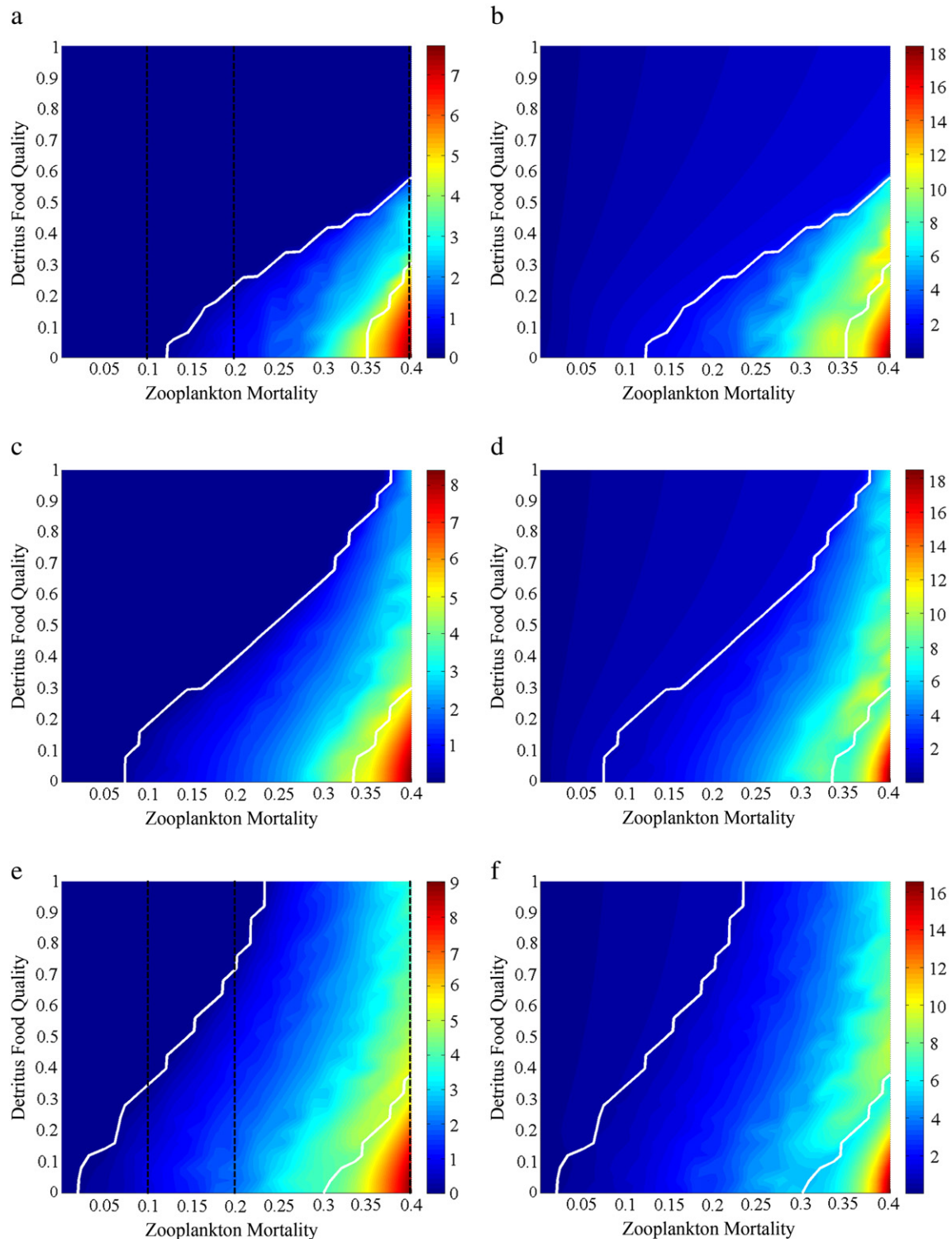


**Fig. 3.** Parameter space exploration between parameters controlling detritus food quality ( $FQ_2$ ) and zooplankton mortality (d). The color map depicts phytoplankton biomass in panels a,c,e and phytoplankton to zooplankton ratio in panels b,d,f; the white contour delineates the oscillatory region(s). Hypolimnetic nutrient concentration is set high ( $PO4_{(hypp)} = 1 \text{ g P m}^{-3}$ ), while light availability ranges from low (panels a and b,  $b = 0.15$ ), to intermediate (panels c and d,  $b = 0.1$ ), and to high (panels e and f,  $b = 0.05$ ) levels. Black dashed lines represent trajectories scanned in Fig. 4.

saddles,<sup>4</sup> limit points in Fig. 5a) are purely academic and will never be experienced. Nonetheless, we produced time series plots of these points, illustrating the jump from one attractor to another (Fig. 5b–d).

<sup>4</sup> Critical point at which eigenanalysis reveals one zero eigenvalue and one negative eigenvalue, balancing the system between a stable attractor and a saddle. The topological structure of such a point is represented by a bowl (global attractor) with opposite ends flattened out (resulting in a taco shell shape). [See also Fig. 4 in Electronic Supplementary Material.]

### 3.4. How intertwined are the effects of intracellular nutrient storage and kinetics on phytoplankton biomass?

The intracellular nutrient regulation of phytoplankton is primarily driven by the minimum amount of nutrients required to reproduce new cells ( $P_{MIN}$ ) and the maximum rate of conversion of intracellular nutrients into storage products/macromolecules ( $P_{MAX}$ ). We tested



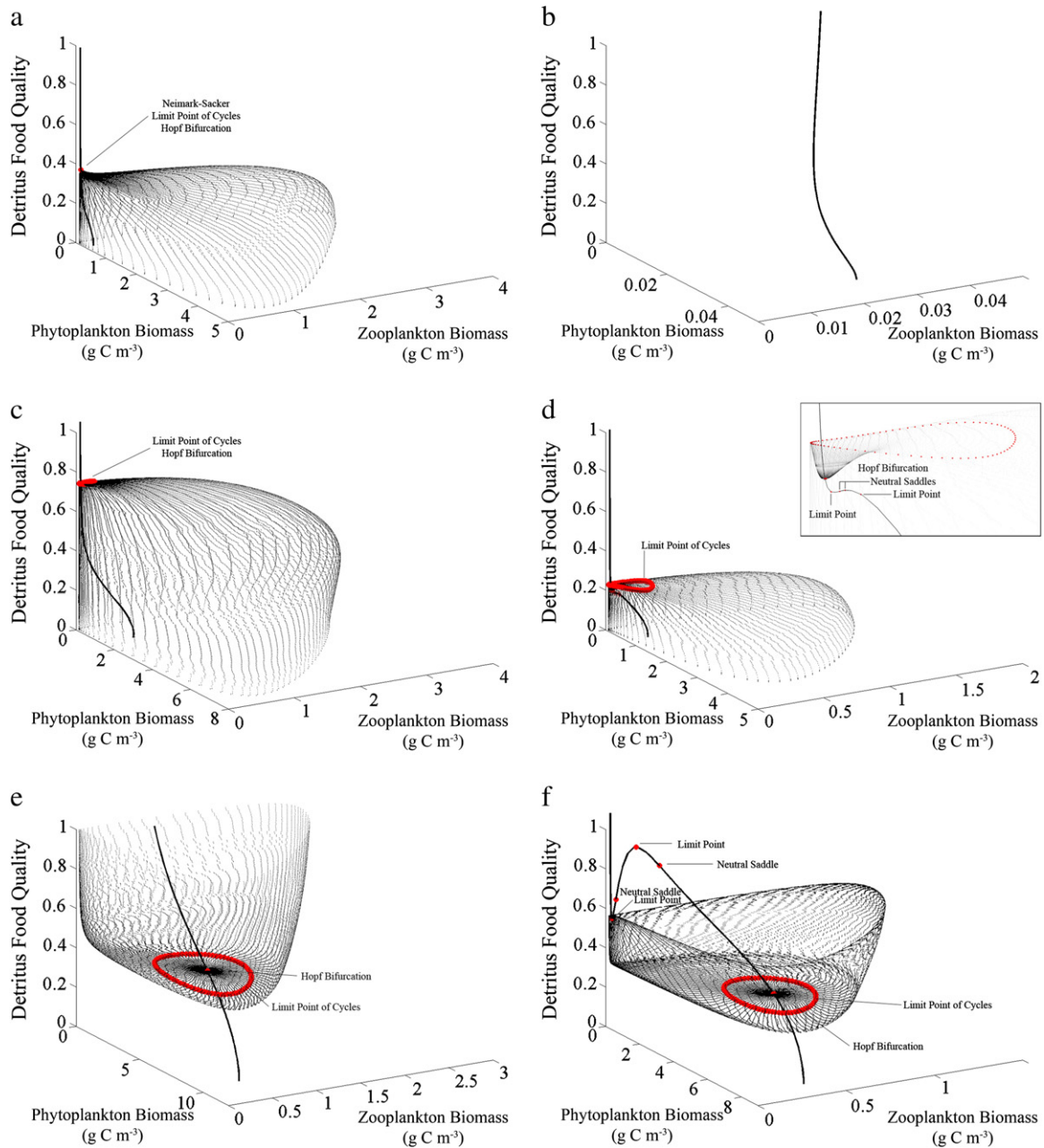


**Fig. 4.** Bifurcation diagrams presenting the phytoplankton and zooplankton limit cycle response to varying detritus food quality ( $FQ_2$ ). Hypolimnetic nutrient concentration is set high ( $PO_4(\text{hyp}) = 1 \text{ g P m}^{-3}$ ). Zooplankton mortality ranged from low ( $d = 0.1 \text{ day}^{-1}$ , panels a,b), to intermediate ( $d = 0.2 \text{ day}^{-1}$ , panels c,d), and to high ( $d = 0.4 \text{ day}^{-1}$ , panels e,f) values. Light availability was altered between high ( $b = 0.05 \text{ m}^{-1}$ , panels a,c,e), and low ( $b = 0.15 \text{ m}^{-1}$ , panels b,d,f) levels.

these two intracellular threshold values against one another in a variety of settings to elucidate their impact on the standing phytoplankton biomass. Low values of  $P_{MIN}$  and  $P_{MAX}$  yielded the highest phytoplankton biomass values when considering high hypolimnetic concentration and low detritus food quality (Fig. 6a). The majority of the phase space sampled was characterized by unforced limit cycles, which disappeared when the hypolimnetic nutrient concentration was lowered to limiting values (Fig. 6b). Under this scenario, the region producing (relatively) large phytoplankton biomass was much narrower and was primarily driven by the minimum nutrient quota. The ecological importance of low  $P_{MIN}$  values in nutrient limiting settings is not surprising, as it reflects a phytoplankton community that has low nutrient requirements for balanced nourishment and growth. Parameterized with high hypolimnetic phosphate concentration and high detritus food quality (Fig. 6c), the system exhibited a response codependent on both minimum and maximum nutrient quotas, although the area where phytoplankton biomass is high

as well as the oscillatory region of the phase space examined were much narrower relative to the scenario in which poor quality detritus was considered. Evidently, the superior zooplankton nutrition obtained from a viable alternative food source plays a role in suppressing phytoplankton. Another key factor that modulates the primary producer intracellular nutrient reserves is the maximum nutrient uptake rate ( $P_{UPMAX}$ ). Yet, our analysis showed that the impact of uptake kinetics on phytoplankton biomass was overshadowed by a low  $P_{MIN}$  under conditions of high hypolimnetic phosphate and low detritus food quality (Fig. 6d). The same pattern was more clearly manifested when low nutrient availability is assumed, and therefore the phytoplankton biomass persists only in regions of extremely low  $P_{MIN}$  (Fig. 6e). Further, the combination of high hypolimnetic nutrient concentration and high detritus food quality limits the magnitude of the phase space in which phytoplankton biomass can flourish (Fig. 6f). The increased detritus food quality narrowed the range of oscillations and the phytoplankton biomass levels due to



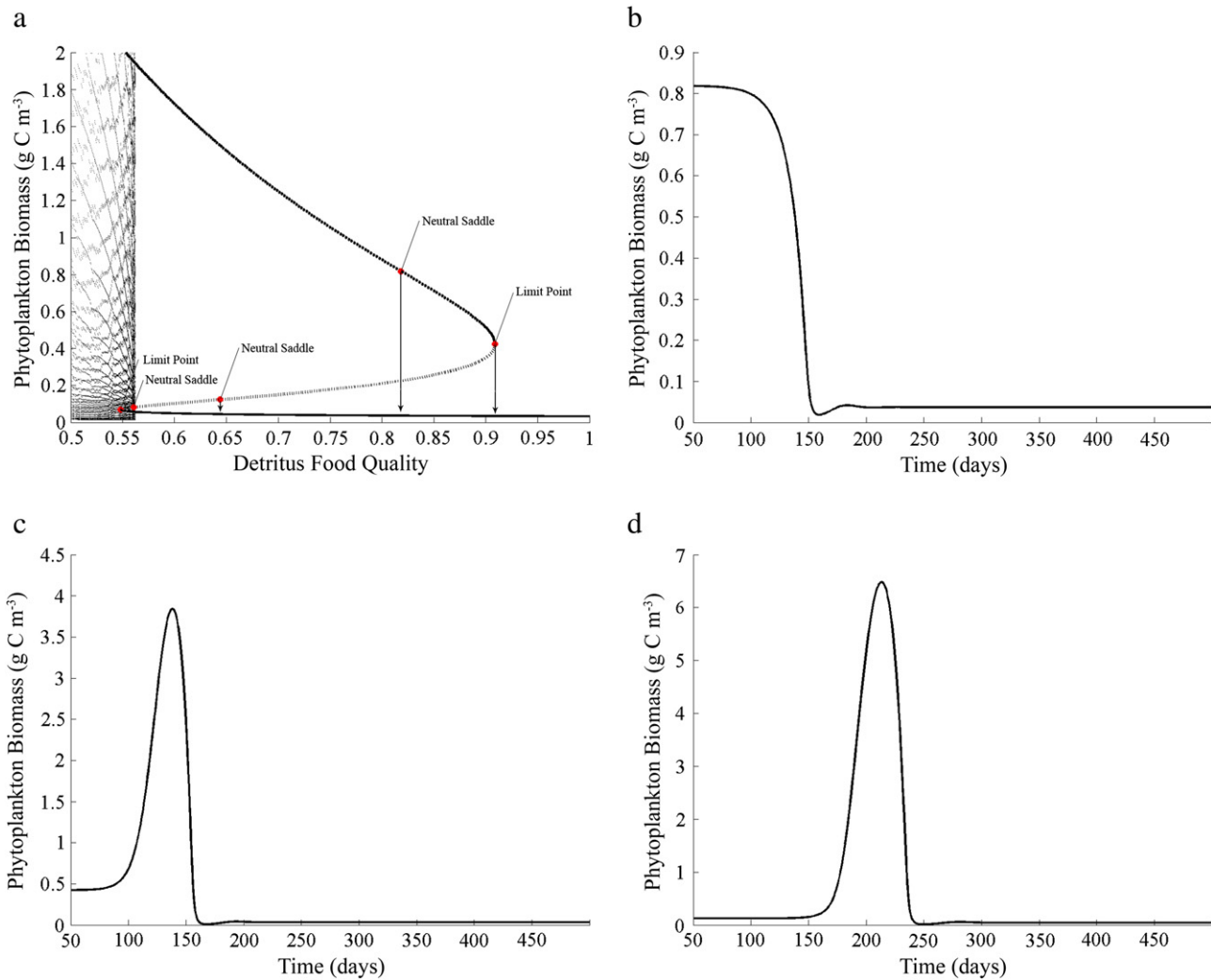


**Fig. 5.** (a) Limit points and neutral saddles arising from the phytoplankton response to varying detritus food quality (as seen in Fig. 4f). Jumps originating from steady/unsteady state equilibrium transition smoothly (b), whereas those originating from imaginary branches demonstrate more abrupt transitions (c,d).

enhanced zooplankton grazing. In the latter scenario, the parameter  $P_{UPMAX}$  demonstrates a distinct pattern of positive covariance with the minimum nutrient quota, whereby the handicap associated with an increasing minimum nutrient quota can be offset by a higher maximum nutrient transport rate at the cell surface.

### 3.5. To what degree can zooplankton somatic nutrient regulations shape phytoplankton biomass dynamics?

The next question addressed was related to the capacity of the factors controlling zooplankton dynamic stoichiometry to shape phytoplankton biomass patterns. The three factors accounted for by our model are the zooplankton minimum and optimal stoichiometric  $P:C$  and the regulatory factor  $N$ . The physiological interpretation of the optimal stoichiometry is the ratio required for optimal zooplankton functioning, while the regulatory factor controls zooplankton homeostatic rigidity. Our simulations provided evidence that consumers with high optimal  $P:C$  and high regulatory factor led to the highest phytoplankton biomass levels as well as to the emergence of oscillatory behavior, whereas phytoplankton was kept to a minimum outside the aforementioned range (Fig. 7a). That is, a firmly homeostatic zooplankton community with high nutrient requirements appears to be malnourished and subsequently exerts minimal control on phytoplankton thereby destabilizing the system. Lowering nutrient availability (via hypolimnetic nutrient concentration) produced similar patterns, but algal biomass was nearly two magnitudes lower and

no oscillations were observed (Fig. 7b). With high nutrient availability and high quality detritus, phytoplankton biomass and limit cycles were restricted to extremely high values of the two parameters considered (Fig. 7c). Generally, the optimal somatic stoichiometry and the regulatory factor seemed to be tightly intertwined, and these strong covariance patterns obfuscate the identification of the primary driving factor in the scenarios tested herein. Interestingly, the third zooplankton stoichiometric parameter – minimum  $P:C$  ratio – was shown to be relatively unimportant on phytoplankton dynamics (Fig. 7d–f), although the ecological ramifications of this result should be interpreted with caution as they may stem from the model parameterization considered in the present analysis.

### 3.6. Are there any underlying interactions when considering both phytoplankton intracellular and zooplankton nutrient regulations/kinetics?

Finally, we examined the interplay between the most influential phytoplankton intracellular and zooplankton somatic nutrient regulatory factors, to illustrate their effects on phytoplankton dynamics. The combination of low  $P_{MIN}$  and high optimal zooplankton  $P:C$  yielded large phytoplankton biomass, while the phase space scrutinized was overwhelmingly characterized by oscillatory behavior (Fig. 8a). Lowering the ambient nutrient availability dramatically altered the patterns observed under a nutrient-rich setting (Fig. 8b). Namely, our simulations

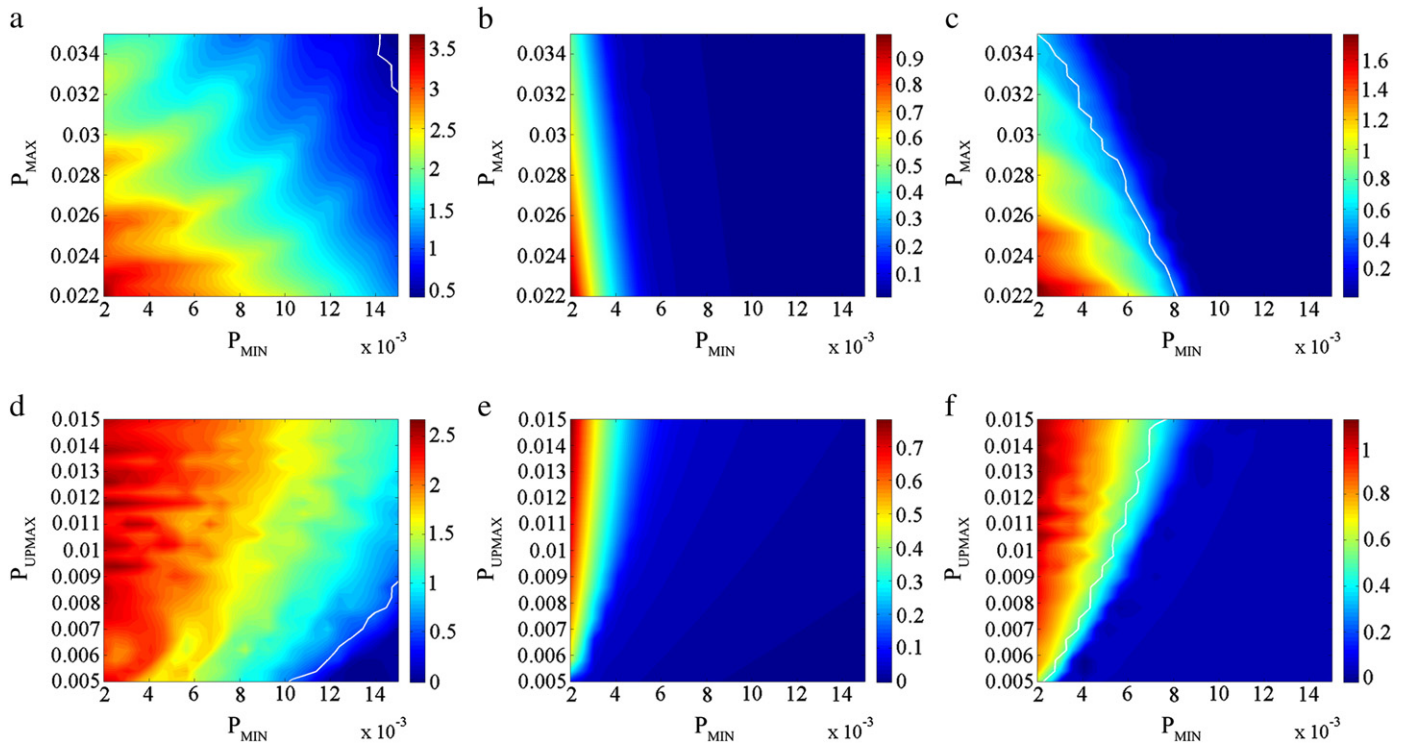


**Fig. 6.** Exploration of parameters controlling intracellular phosphorus storage: minimum quota ( $P_{min}$ ) and maximum quota ( $P_{max}$ ) (a,b,c),  $P_{min}$  and maximum nutrient uptake rate ( $P_{upmax}$ ) (d,e,f). Light availability is held high, and zooplankton mortality is intermediate. The scenarios tested include low detritus food quality and high hypolimnetic nutrient concentration (a and d), low detritus food quality and low hypolimnetic nutrient concentration (b and e), high detritus food quality and high hypolimnetic nutrient concentration (c and f). A white contour delineates oscillatory region(s).

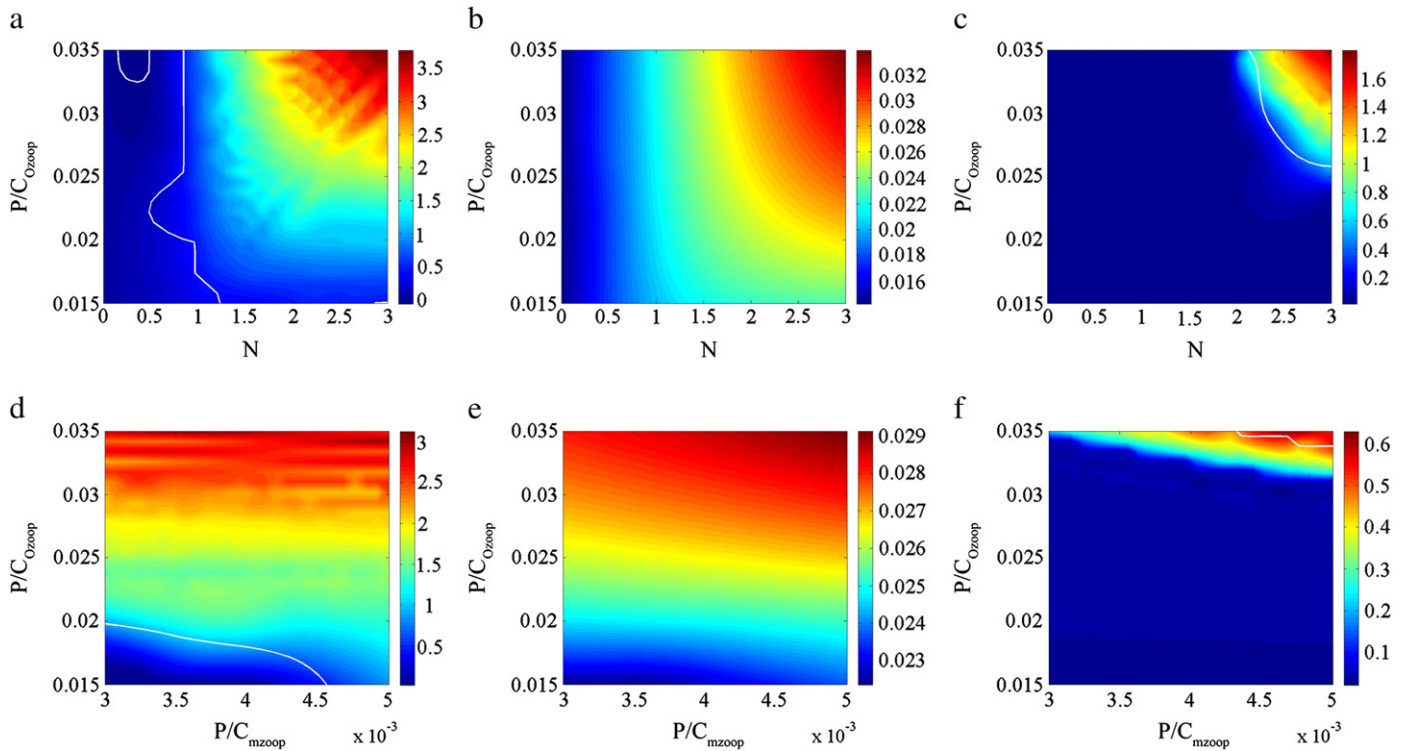


**Fig. 7.** Exploration of parameters controlling zooplankton stoichiometry: optimal somatic P:C ( $PC_{Ozooop}$ ) and the regulatory coefficient ( $N$ ) (a,b,c),  $PC_{Ozooop}$  and minimum somatic P:C ( $PC_{MINzooop}$ ) (d,e,f). Light availability is held high, and zooplankton mortality is intermediate. The scenarios tested include low detritus food quality and high hypolimnetic nutrient concentration (a and d), low detritus food quality and low hypolimnetic nutrient concentration (b and e), high detritus food quality and high hypolimnetic nutrient concentration (c and f). A white contour delineates oscillatory region(s).

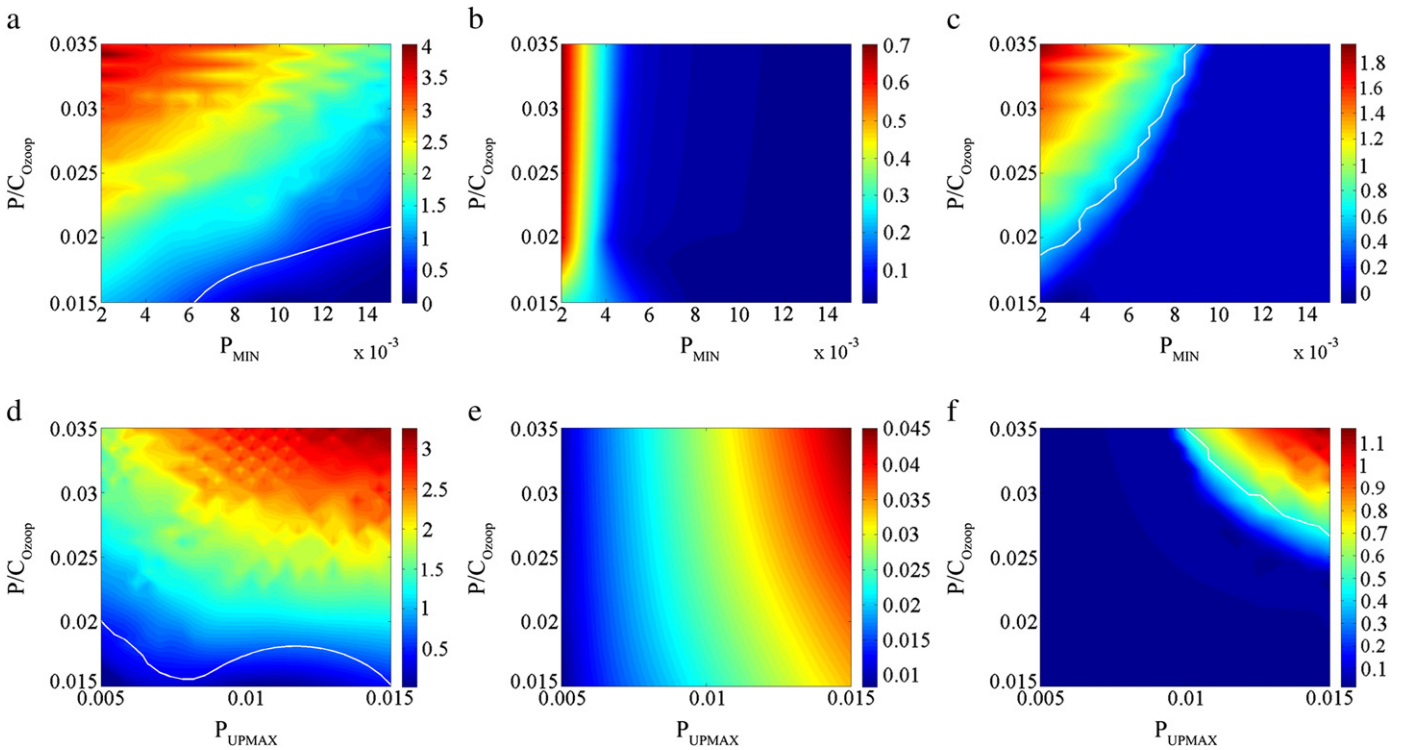


**Fig. 8.** Exploration combining factors of intracellular storage and zooplankton stoichiometric regulation:  $P_{min}$  and  $PC_{Ozoop}$  (a,b,c),  $P_{upmax}$  and  $PC_{Ozoop}$  (d,e,f). Light availability is held high, and zooplankton mortality is intermediate. The scenarios tested include low detritus food quality and high hypolimnetic nutrient concentration (a and d), low detritus food quality and low hypolimnetic nutrient concentration (b and e), high detritus food quality and high hypolimnetic nutrient concentration (c and f). A white contour delineates oscillatory region(s).

showed that under severe nutrient stress, phytoplankton is predominantly bottom-up controlled and therefore the minimum nutrient quota is the primary driving factor. Similar to our first experiment, the system exhibits a distinct covariance pattern between algal minimum quota and zooplankton optimal stoichiometry, when both nutrient availability and detritus food quality are high (Fig. 8c). Yet, we also note that the reliance upon a second food source in the latter setting increases zooplankton grazing and subsequently narrows the range in which phytoplankton activity occurs. The most striking observations were made from the pairwise comparison of the optimal somatic stoichiometry and maximum uptake rate (Fig. 8d–f). In a nutrient rich setting, given  $P_{UPMAX}$  was sufficiently high, optimal stoichiometry was predominantly controlling phytoplankton biomass (Fig. 8d). Reducing nutrient availability, however, shifted emphasis to the maximum uptake rate (Fig. 8e). This switch from top-down control (when nutrient availability is high) to bottom-up (when nutrients are limited) is consistent with our previous findings ( $P_{MIN}$  vs.  $P/C_{Ozoop}$ ). Consistent with patterns delineated in previous experiments, high nutrient availability and high detritus food quality limited the oscillatory region and the phytoplankton biomass levels experienced in the system (Fig. 8f).

#### 4. Discussion

**Phytoplankton intracellular storage capacity:** Many of the recent empirical findings related to the factors that drive the flow of mass and energy in the phytoplankton–zooplankton interface have not been explicitly considered by contemporary modeling studies. The present analysis aimed to fill this gap through the development of an upgraded NPZD model, in which the primary producer has variant intracellular nutrient reserves, and the grazer is characterized by a quasi-dynamic stoichiometry and fully dynamic assimilation efficiency. Our model is on par with the conclusion drawn by Sanudo-Wilhelmy et al. (2004), which challenged the notion of a globally constant stoichiometry across the lower food web, suggesting that the stoichiometric ratios vary with the algal nutrient

status and taxonomic affiliation. Klausmeier et al. (2004) asserted that this variability is primarily associated with the internal storage of nutrients, whereas the functional machinery of a cell has a nearly constant chemical composition. The Redfield ratio appears to be an accurate approximation when comparing total-P to N and C, but inaccurate when considering the intracellular reserves (Sanudo-Wilhelmy et al., 2004). Apparently, the existence of two distinct phosphorus pools in phytoplankton renders support to the notion that P uptake is a two-step kinetic process, whereby P is first adsorbed to the cell surface and then is internalized (Flynn, 2009; Hudson and Morel, 1993). One of the pillars of our analysis is this disconnect between phytoplankton uptake and assimilation, and the postulated ability of the pertinent subcellular processes to maintain a positive net growth rate is relayed to the population level.

Of the parameters controlling intracellular phosphorus storage capacity, our modeling study pinpoints the minimum amount of phosphorus required for the basic cellular metabolic processes and production of new cells ( $P_{MIN}$ ) to be the single most important governing factor of phytoplankton abundance when conditions of low ambient phosphorus are experienced. This result is not surprising, as earlier work from Grover (1991) similarly showed that a decrease in the minimum nutrient quota provides competitive advantage in both equilibrium and non-equilibrium habitats. Likewise, Arhonditsis and Brett (2005a) and later Zhao et al. (2008a) showed that the predominant role of this parameter in the interspecific competition is also manifested with complex models, in which several – often contrasting – mechanisms (e.g., vertical mixing, herbivory, seasonal forcing) are explicitly modeled. The additional undertaking here was the attempt to elucidate the suite of abiotic conditions, stoichiometric strategies, and trophic interactions that may modulate the impact of this parameter. In particular, we note that an increasing maximum bound on the intracellular phosphorus can partly negate the advantages gained by a low value of the minimum phosphorus quota, suggesting that a higher maximum rate of conversion of the intracellular nutrients into storage products/macromolecules (i.e., the fabric of organelles and other complex cellular components) can result in reduced



growth even when the ambient phosphorus levels are relatively high (Zhao et al., 2008a). Consistent with our results, Grover (1991) found that a lower  $P_{MAX}$  is always advantageous in equilibrium habitats, whereas species with higher upper  $P$  bound may dominate the phytoplankton community in non-equilibrium conditions depending on the magnitude and period of the intermittent nutrient pulses. Although beyond the scope of the present study, our feedback term  $P_{FB}$  (Table 1) can potentially reproduce patterns of phytoplankton biomass increase when high  $P_{MAX}$  values are considered, as it prolongs the rapid uptake capability and therefore allows phytoplankton to capitalize on a greater fraction of the nutrient pulses (Grover, 1991; Turpin, 1988).

The negative relationship between phytoplankton abundance and the lower/upper bounds of intracellular phosphorus can also be viewed from a different angle that involves the causal association between internal nutrient quotas and algal cell morphology. As previously mentioned, the combination of low  $P_{MIN}$  and  $P_{MAX}$  values always results in greater phytoplankton biomass levels, and thus reinforces the notion of a positive influence of the small cells, typically possessing lower maximum and minimum nutrient quotas, on algal growth capacity (Grover, 1991; Jiang et al., 2005; Thingstad et al., 2005; Yoshiyama and Klausmeier, 2008). Yet, our analysis also shows that the same phytoplankton parameterization can lead to the emergence of unforced oscillations, depending on the prevailing ambient nutrient levels and strength of the top-down control. While the likelihood of the intracellular storage capacity to act as a destabilizing force in planktonic food web systems is certainly intriguing (and largely unexplored), we highlight two additional aspects of the cell morphology that may be indispensable for objectively assessing its ramifications on the primary producer–grazer interactions. First, the role of the cell shape (e.g., spherical vs. elongated) appears to be as important as the cell size, and the explicit consideration of allometric relations between physiological processes and cell morphological characteristics may be critical to examine the broader range of dynamics associated with this planktonic system (Grover, 1989a,b; Reynolds, 2006). Second, existing evidence suggests that a complex interplay between nutrient limitation and cell morphology (e.g., thickening of cell walls) can modulate the grazing resistance in phytoplankton (DeMott and Tessier, 2002; Ravet and Brett, 2006; Van Donk et al., 1997). Thus, a logical next step may be to relax our assumption of conditional independence between zooplankton palatability for phytoplankton ( $FQ_I$ ) and internal nutrient quotas, and subsequently examine the broader implications of a direct (or indirect) causal connection between the two parameters (DeMott, 1982, 1986; DeMott et al., 2004; Ferrão Filho et al., 2005; Ravet and Brett, 2006).

According to our analysis, another key process that appears to regulate the internal nutrient content is the maximum transport rate at the cell surface ( $P_{UPMAX}$ ). Although the present model is certainly simpler than recent multi-step (i.e., diffusive transport, membrane uptake, and cellular catalysis) mathematical representations (Yoshiyama and Klausmeier, 2008), we found that the region of high phytoplankton biomass and oscillatory behavior is distinctly extended when high  $P_{UPMAX}$  values are assumed. Based on our model predictions, we can also infer that when an algal community on average possesses the attributes of our phytoplankton characterization (e.g., low maximum growth and metabolic rates, high half saturation for phosphorus uptake, low food quality) and is also associated with higher  $P_{UPMAX}$  values, planktonic food webs are susceptible to instability patterns under nutrient enrichment conditions (Fig. 6d and f); a scenario that may not be unrealistic, if the assumption of a positive co-variance between  $P_{UPMAX}$  and the half saturation for phosphorus uptake ( $K_p$ ) holds true (Crowley, 1975; Grover, 1991). The kinetics of transport in conjunction with the intracellular assimilation processes have received considerable attention in the literature, and earlier work by Turpin (1988) hypothesized a trade-off between the kinetics of transport and the assimilation rates arising from the limited amount of protein per cell that can be allocated between the two generic processes. Drawing parallels between the present study and Grover's (1991) variable-internal-stores model, the implications of this hypothesis can be

examined by postulating a negative relationship between the maximum nutrient transport rate and the maximum nutrient quota. In particular, a phytoplankton specification with high  $P_{UPMAX}$  and low  $P_{MAX}$  depicts a strategist that first strives for rapid nutrient uptake, thereby eliminating the likelihood of limitation due to nutrient transport. Yet, as  $P_{INT}$  gradually approaches  $P_{MAX}$ , the uptake rate would be reduced, while the production of new cells will tend towards the maximum growth potential, representing the transition to limitation by the assimilation rate. The latter parameterization will likely be advantageous in nutrient-limiting environments, where rapid transport is more beneficial than rapid assimilation. Numerical simulations with low hypolimnetic nutrient levels (not presented here) showed that such autotrophic community can indeed overcome the scarcity of nutrients and the system demonstrates the highest phytoplankton-to-zooplankton ratios.

**Zooplankton stoichiometry:** Recent empirical evidence suggests that the assumption of strict elemental homeostasis does not always explain *Daphnia* dynamics in  $P$ -deficient environments (Ferrão Filho et al., 2007). To examine the implications of a flexible grazer stoichiometry, Mulder and Bowden (2007) introduced a power–curve relationship between zooplankton ( $P/C_{zoop}$ ) and seston ( $P_i$ ) carbon to phosphorus ratios, which confines the variability of the phosphorus somatic content within the  $P/C_{Ozoop}$  and  $P/C_{MINzoop}$  bounds. Our analysis primarily highlights the importance of the interplay between optimal stoichiometric  $P:C$  and the regulatory factor  $N$  that controls zooplankton homeostatic rigidity. Namely, the predominance of  $P$ -rich herbivores characterized by tight homeostasis (i.e., high optimal  $P:C$  and  $N$  values) can potentially lead to high phytoplankton abundance, high phytoplankton-to-zooplankton ratios, and acceleration of oscillatory behavior. A plausible explanation for these patterns is that our model postulates a two-step mechanism through which zooplankton homeostasis is maintained:

- (i) Animals remove nutrient elements in closer proportion to their somatic ratios than to the seston elemental ratio during the digestion and assimilation process (Arhonditsis and Brett, 2005b; Zhao et al., 2008b). Thus, when zooplankton experiences  $P$ -deficient diets relative to its somatic requirements, strict elemental homeostasis is maintained through excretion of the excess carbon or decrease of carbon assimilation, e.g., the  $a_C$  term in our model (DeMott et al., 1998; Sterner, 1997). Such strategy gradually leads to zooplankton growth reduction which in turn alleviates phytoplankton from herbivorous grazing. This process may be predominant in habitats with high food availability, in which the presence of alternative nutritionally reliable food sources can also determine the zooplankton sensitivity to  $P$  deficient diets, e.g., the differences between the phytoplankton response in Fig. 7a and c (see also following discussion).
- (ii) Once the somatic requirements are met, the stoichiometric signature of the excreted material is strictly determined by the consumer elemental composition. Based on this conceptualization, the  $P$ -rich animals (e.g., *Daphnia*) should contribute a significant proportion of the excess carbon during their feeding (high  $C:P$ ), but subsequently have higher release rates of phosphorus per unit of biomass due to excretion of their metabolic by-products or decomposition of dead material, e.g., tissues, carapaces (low  $C:P$ ), contributing more to the internal fuelling of the autotrophic community. According to our model predictions, the relative contribution of this pathway becomes more significant in resource-limiting environments, typically demonstrating greater dependence on internal nutrient subsidies (Fig. 7b).

Yet, in “real-world” conditions, nutrient recycling can considerably vary with the composition of the zooplankton community, and existing evidence suggests that rotifers usually have higher rates of phosphorus excretion per unit of biomass relative to copepods or  $P$ -rich cladocerans (Ejsmont-Karabin et al., 2004; Gulati et al., 1989; Kowalewska-Madura et al., 2007; Teubner et al., 2003). Further, the alternative

hypothesis proposed is that homeostatic regulation is primarily mediated by post-absorptive mechanisms and therefore *P*-deficient diets can lead to a dramatic reduction of the consumer *P* excretion/respiration rates and maximization of the *P* assimilation efficiency (Elser and Urabe, 1999). In this case, although some animals can excrete in organic forms (e.g., urea), most nutrients are recycled in inorganic forms (e.g., ammonia, phosphate) and thus the excretion rates are tightly related to the ambient nutrient levels. Experimental work in laboratory settings appears to render support to the latter hypothesis (Darchambeau et al., 2003). On the other hand, the robustness of its predictions at an ecosystem scale remains largely unexplored, and model parameterizations that assign higher portion of the recycled material into the dissolved-phase pool tend to predict unrealistically high levels of the non-limiting elements (ammonium) in the water column (Arhonditsis and Brett, 2005b). Because the relative importance of the pre- vs. post-absorption mechanisms of food processing and their ramifications on ecosystem functioning have not been unequivocally addressed in the contemporary literature (Arhonditsis and Brett, 2005b; Darchambeau et al., 2003; DeMott et al., 1998; Elser and Foster, 1998; Urabe et al., 2002; Zhao et al., 2008b), we caution that the representation of the stoichiometric variability of consumer-driven nutrient recycling is one of the aspects of the current generation of plankton models that needs to be revisited.

**Detritus food quality:** In an earlier study, Perhar and Arhonditsis (2009) advocated the somewhat provocative notion that the algal food quality may be the single most important factor responsible for the two alternative states of planktonic food webs, i.e., the state of an inverted food web pyramid, in which relatively low phytoplankton biomass can sustain high zooplankton and subsequently fish production, and the least desirable hypereutrophic state, in which high primary producer biomass coexists with low production at the higher trophic levels. Our present results though challenge the latter scenario showing that such transition is dependent upon the presence of an alternative reliable food source, detritus, which appears to primarily shape the food web architecture when phytoplankton food quality is low. The profitability of detritus can apparently prevent the minimum abundance of zooplankton from falling below certain threshold levels, and thus increases the resilience of the primary producer–grazer systems (Genkai-Kato and Yamamura, 1999; Perhar and Arhonditsis, 2009). In a modeling context, this notion is far from novel and it has been shown the explicit consideration of a detritus pool tends to eliminate (or drastically reduce) the unforced limit cycles and chaos exhibited by simpler models (Edwards, 2001). The empirical underpinning of the role of detritus as an ecosystem stabilizer was provided by Wetzel (1995), who argued that most of the particulate matter in lakes is relatively recalcitrant, thereby acting as a “muffler” that dampens the phytoplankton–zooplankton oscillations. Yet, counter to our current understanding, the present modeling analysis also shows that the impact of detritus on ecosystem functioning is not as straightforward as usually deemed. If zooplankton encounters inferior algal food quality, then detritus can be responsible for abrupt shifts to alternative states, depending on the levels of other important ecological factors (light or nutrient availability, zooplankton mortality/higher predation). In technical terms, there are multiple attractors and the impact of detritus food quality on the basins of attraction that determines which attractor prevails depends on the interactions between the abiotic conditions and biotic components of the habitat (Figs. 4 and 5).

Given the absence of an exogenous carbon source in our modeling experiments, our detritus pool is largely of biogenic origin, and therefore the question arising is what is really known with regards to the capacity of autochthonous detritus to contribute to overall ecosystem productivity? Existing empirical and modeling evidence suggests that bacteria preferentially use phytoplankton-derived *DOC* and convert this carbon to bacteria biomass at a greater efficiency than they do with allochthonous *DOC*; even in net heterotrophic ecosystems, where the utilization of exogenous carbon by bacteria is high (Karlsson et al., 2001; Kritzberg et al., 2005; Tranvik, 1988). Based on these patterns, Kritzberg et al. (2005) argued

that most of the allochthonous carbon assimilated by bacteria is unlikely to be transferred to the higher trophic levels. Furthermore, Karlsson (2007) proposed an uncoupling between anabolic and catabolic metabolism in the lakes, whereby allochthonous carbon may primarily contribute to catabolic metabolism, while autochthonous carbon is more closely associated with the anabolic processes. Likewise, Brett et al. (2009) argued that the phytoplankton component of zooplankton diet is selectively used for production of new somatic material, whereas the lower-quality terrestrial particulate matter may be catabolized for metabolic energy demands. The same study also hypothesized that the availability of high food quality phytoplankton regulates the incorporation of low-quality allochthonous carbon into pelagic food web production. In a way, the latter assertion has conceptual similarities with one of our findings, in that the presence of a higher quality food sources in the system (i.e., autochthonous detritus) facilitates zooplankton to more effectively control the other food source (i.e., a cyanobacterium-like phytoplankton) despite its inferior nutritional quality.

In pursuit of “opening the black box” of the factors that modulate the strength of the phytoplankton–zooplankton interactions, we have progressed from adding an alternate food source and considering both food quantity and quality (Perhar and Arhonditsis, 2009), to the dynamic intracellular and somatic approach of the current study. One of the emerging imperatives in aquatic ecosystem modeling is the mathematical representation of the factors that more faithfully depict seston food quality and mass/energy flow through the plant–animal interface. In this regard, HUFAs content may be critical in further advancing our understanding of zooplankton assimilation efficiency. Many empirical studies have been published on algal HUFAs (e.g., Müller-Navarra, 1995), but integration into plankton population models remains almost non-existent. Our current study illustrates the manner in which phytoplankton intracellular reserves may be considered by a plankton population model and still predict ecologically sound patterns that cannot be reproduced by simpler approaches. Acknowledging that organisms are built out of permanent (structure) and non-permanent (reserves) components, and explicitly treating the mobility of essential fatty acids and phosphorus between the two distinct pools may be the counterbalance (to existing empirical studies) required to bring explicit trophic energy transfer efficiencies to the forefront of modeling practices (Kooijman, 2001).

## Acknowledgments

This project has received funding support from the Natural Sciences and Engineering Research Council of Canada through a Doctoral Scholarship awarded to Gurbir Perhar and a Discovery Grant awarded to George Arhonditsis.

## Appendix A. Supplementary data

Supplementary data to this article can be found online at <http://dx.doi.org/10.1016/j.ecoinf.2012.06.002>.

## References

- Arhonditsis, G.B., Brett, M.T., 2005a. Eutrophication model for Lake Washington (USA) Part I. Model description and sensitivity analysis. *Ecological Modelling* 187, 140–178.
- Arhonditsis, G.B., Brett, M.T., 2005b. Eutrophication model for Lake Washington (USA) Part II. Model calibration and system dynamics analysis. *Ecological Modelling* 187, 179–200.
- Brett, M.T., Müller-Navarra, D.C., Park, S.K., 2000. Empirical analysis of the effect of phosphorus limitation on algal food quality for freshwater zooplankton. *Limnology and Oceanography* 45 (7), 1564–1575.
- Brett, M.T., Müller-Navarra, D.C., Ballantyne, A.P., Ravet, J.L., Goldman, C.R., 2006. *Daphnia* fatty acid composition reflects that of their diet. *Limnology and Oceanography* 51 (5), 2428–2437.
- Brett, M.T., Kainz, M.J., Taipale, S.J., Seshan, H., 2009. Phytoplankton, not allochthonous carbon, sustains herbivorous zooplankton production. *Proceedings of the National Academy of Sciences of the United States of America* 106 (50), 21197–21201.
- Crowley, P.H., 1975. Natural selection and the Michaelis constant. *Journal of Theoretical Biology* 50, 461–475.

- Danielsdottir, M.G., Brett, M.T., Arhonditsis, G.B., 2007. Phytoplankton food quality control of planktonic food web processes. *Hydrobiologia* 589, 29–41.
- Darchambeau, F., Faerøvig, P.J., Hessen, D.O., 2003. How *Daphnia* copes with excess carbon in its food. *Oecologia* 136, 336–346.
- DeMott, W.R., 1982. Feeding selectivities and relative ingestion rates of *Daphnia* and *Bosmina*. *Limnology and Oceanography* 27 (3), 518–527.
- DeMott, W.R., 1986. The role of taste in food selection by freshwater zooplankton. *Oecologia* 69 (3), 334–340.
- DeMott, W.R., Müller-Navarra, D.C., 1997. The importance of highly unsaturated fatty acids in zooplankton nutrition: Evidence from experiments with *Daphnia*, a cyanobacterium and lipid emulsions. *Freshwater Biology* 38, 649–664.
- DeMott, W.R., Pape, B.J., 2005. Stoichiometry in an ecological context: testing for links between *Daphnia* P-content, growth rate and habitat preference. *Oecologia* 142, 20–27.
- DeMott, W.R., Tessier, A.J., 2002. Stoichiometric constraints vs. algal defenses: testing mechanisms of zooplankton food limitation. *Ecology* 83 (12), 3426–3433.
- DeMott, W.R., Gulati, R.D., Siewertsen, K., 1998. Effects of phosphorus-deficient diets on the carbon and phosphorus balance of *Daphnia magna*. *Limnology and Oceanography* 43 (6), 1147–1161.
- DeMott, W.R., Pape, B.J., Tessier, A.J., 2004. Patterns and sources of variation in *Daphnia* phosphorus content in nature. *Aquatic Ecology* 38, 433–440.
- Dhooge, A., Govaerts, W., Kuznetsov, Y.A., 2003. Numerical continuation of fold bifurcations of limit cycles in MATCONT. *Lecture Notes in Computer Science* 2657, 701–710.
- Droop, M.R., 1968. Vitamin B12 and marine ecology. IV. The kinetics of uptake, growth and inhibition in *Monochrysis lutheri*. *Journal of the Marine Biological Association of the United Kingdom* 48, 689–733.
- Edwards, A.M., 2001. Adding detritus to a nutrient–phytoplankton–zooplankton model: a dynamical-systems approach. *Journal of Plankton Research* 23 (4), 389–413.
- Edwards, A.M., Yool, A., 2000. The role of higher predation in planktonic population models. *Journal of Plankton Research* 22 (6), 1085–1112.
- Ejsmont-Karabin, J., Gorelysheva, Z., Kalinowska, K., Węgleńska, T., 2004. Role of zooplankton (ciliate, rotifer and crustacean) in phosphorus removal from cycling: lakes of the River Jorka watershed (Masuria Lakeland, Poland). *Polish Journal of Ecology* 52 (3), 275–284.
- Elser, J.J., Foster, D.K., 1998. N:P stoichiometry of sedimentation in lakes of the Canadian shield: relationships with seston and zooplankton elemental composition. *Ecoscience* 5 (1), 56–63.
- Elser, J.J., Urabe, J., 1999. The stoichiometry of consumer-driven nutrient recycling: theory, observations, and consequences. *Ecology* 80 (3), 735–751.
- Elser, J.J., Elser, M.M., MacKay, N.A., Carpenter, S.R., 1988. Zooplankton-mediated transitions between N- and P-limited algal growth. *Limnology and Oceanography* 33 (1), 1–14.
- Ferrão Filho, A.D.S., DeMott, W.R., Tessier, A.J., 2005. Responses of tropical cladocerans to a gradient of resource quality. *Freshwater Biology* 50, 954–964.
- Ferrão Filho, A.D.S., Tessier, A.J., DeMott, W.R., 2007. Sensitivity of herbivorous zooplankton to phosphorus-deficient diets: testing stoichiometric theory and the growth rate hypothesis. *Limnology and Oceanography* 52 (1), 407–415.
- Flynn, K.J., 2009. Going for the slow burn: why should possession of a low maximum growth rate by advantageous for microalgae? *Plant Ecology & Diversity* 2 (2), 179–189.
- Genkai-Kato, M., Yamamura, N., 1999. Unpalatable prey resolves the paradox of enrichment. *Pbios* 266 (1425), 1215–1219.
- Grover, J.P., 1989a. Phosphorus-dependent growth kinetics of 11 species of freshwater algae. *Limnology and Oceanography* 34 (2), 341–348.
- Grover, J.P., 1989b. Effects of Si:P supply ratio, supply variability, and selective grazing in the plankton: an experiment with a natural algal and protistan assemblage. *Limnology and Oceanography* 34 (2), 349–367.
- Grover, J.P., 1991. Resource competition in a variable environment: phytoplankton growing according to the variable-internal-stores model. *The American Naturalist* 138 (4), 811–835.
- Guisande, C., Riveiro, I., Maneiro, I., 2000. Comparisons among the amino acid composition of females, eggs and food to determine the relative importance of food quantity and food quality to copepod reproduction. *Marine Ecology Progress Series* 202, 135–142.
- Gulati, R.D., Ejsmontkarabin, J., Rooth, J., Siewertsen, K., 1989. A laboratory study of phosphorus and nitrogen-excretion of *Euchlanis-Dilatata-Lucksiana*. *Hydrobiologia* 186, 347–354.
- Hudson, R.J.M., Morel, F.M.M., 1992. Trace metal transport by marine microorganisms: implications of metal coordination kinetics. *Deep Sea Research* 40 (1), 129–150.
- Jiang, L., Schofield, O.M.E., Falkowski, P.G., 2005. Adaptive evolution of phytoplankton cell size. *The American Naturalist* 166 (4), 496–505.
- Karlsson, J., 2007. Different carbon support for respiration and secondary production in unproductive lakes. *Oikos* 116 (10), 1691–1696.
- Karlsson, J., Jonsson, A., Jansson, M., 2001. Bacterioplankton production in lakes along an altitude gradient in the subarctic North of Sweden. *Microbial Ecology* 42, 372–382.
- Klausmeier, C.A., Litchman, E., Levin, S.A., 2004. Phytoplankton growth and stoichiometry under multiple nutrient limitation. *Limnology and Oceanography* 49 (4:2), 1463–1470.
- Kooijman, S.A.L.M., 2001. Quantitative aspects of metabolic organization: a discussion of concepts. *Philosophical Transactions of The Royal Society B* 356 (1407), 331–349.
- Kowalewska-Madura, K., Goldyn, R., Szyper, H., 2007. Zooplankton phosphorus excretion in Swarzedzkie Lake (Western Poland) and its influence on phytoplankton. *Oceanological and Hydrobiological Studies* 36, 3–16.
- Kritzberg, E.S., Cole, J.J., Pace, M.M., Granéli, W., 2005. Does autochthonous primary production drive variability in bacterial metabolism and growth efficiency in lakes dominated by terrestrial C inputs? *Aquatic Microbial Ecology* 38, 103–111.
- Lehman, J.T., 1984. Grazing, nutrient release, and their impacts on the structures of phytoplankton communities. In: Meyers, D.G., Strickler, J.R. (Eds.), *Trophic Interactions within Aquatic Ecosystems*. AAAS Selected Symposium 85. Westview Press, Boulder, pp. 49–72.
- Loladze, I., Kuang, Y., Elser, J.J., 2000. Stoichiometry in producer–grazer systems: linking energy flow with elemental cycling. *Bulletin of Mathematical Biology* 62, 1137–1162.
- Mulder, K., Bowden, W.B., 2007. Organismal stoichiometry and the adaptive advantage of variable nutrient use and production efficiency in *Daphnia*. *Ecological Modelling* 202, 427–440.
- Müller-Navarra, D.C., 1995. Biochemical versus mineral limitation in daphnia. *Limnology and Oceanography* 40 (7), 1209–1214.
- Perhar, G., Arhonditsis, G.B., 2009. The effects of seston food quality on planktonic food web patterns. *Ecological Modelling* 220, 805–820.
- Ravet, J.L., Brett, M.T., 2006. Phytoplankton essential fatty acid and phosphorus content constraints on *Daphnia* somatic growth and reproduction. *Limnology and Oceanography* 51 (5), 2438–2452.
- Reynolds, C.S., 2006. *The Ecology of Phytoplankton*. Cambridge University Press, Cambridge. 535 pp.
- Sanudo-Wilhelmy, S.A., Tovar-Sanchez, A., Fu, F.X., Capone, D.G., Carpenter, E.J., Hutchins, D.A., 2004. The impact of surface-adsorbed phosphorus on phytoplankton Redfield stoichiometry. *Nature* 432, 897–901.
- Smyntek, P.M., Teece, M.A., Schulz, K.L., Storch, A.J., 2008. Taxonomic differences in the essential fatty acid composition of groups of freshwater zooplankton relate to reproductive demands and generation time. *Freshwater Biology* 53, 1768–1782.
- Stern, R.W., 1990. The ratio of nitrogen to phosphorus resupplied by herbivores: zooplankton and the algal competitive arena. *The American Naturalist* 136 (2), 209–229.
- Stern, R.W., 1997. Modelling interactions of food quality and quantity in homeostatic consumers. *Freshwater Biology* 38, 473–481.
- Teubner, K., Crosbie, N.D., Donabaum, K., Kabas, Q., Kirschner, A.K.T., Pfister, G., Salbrechter, M., Dokulil, M.T., 2003. Enhanced phosphorus accumulation efficiency by the pelagic community at reduced phosphorus supply: a lake experiment from bacteria to metazoan zooplankton. *Limnology and Oceanography* 48 (3), 1141–1149.
- Thingstad, T.F., Øvreås, L., Egge, J.K., Løvdal, T., Heldal, M., 2005. Use of non-limiting substrates to increase size: a generic strategy to simultaneously optimize uptake and minimize predation in pelagic osmotrophs? *Ecology Letters* 8, 675–682.
- Tranvik, L.J., 1988. Availability of dissolved organic carbon for planktonic bacteria in oligotrophic lakes of differing humic content. *Microbial Ecology* 16 (3), 311–322.
- Turpin, D.H., 1988. Physiological mechanisms in phytoplankton resource competition. In: Sandgren, C.D. (Ed.), *Growth and Reproductive Strategies of Freshwater Phytoplankton*. Cambridge University Press, New York, pp. 316–368.
- Urabe, J., Elser, J.J., Kyle, M., Yoshida, T., Sekino, T., Kawabata, Z., 2002. Herbivorous animals can mitigate unfavorable ratios of energy and material supplies by enhancing nutrient cycling. *Ecology Letters* 5, 177–185.
- Van Donk, E., Hessen, D.O., 1993. Grazing resistance in nutrient-stressed phytoplankton. *Oecologia* 93 (4), 508–511.
- Van Donk, E., Lurling, M., Hessen, D.O., Lokhorst, G.M., 1997. Altered cell wall morphology in nutrient-deficient phytoplankton and its impact on grazers. *Limnology and Oceanography* 42 (2), 357–364.
- Wacker, A., Martin-Creuzburg, D., 2007. Allocation of essential lipids in *Daphnia magna* during exposure to poor food quality. *Functional Ecology* 21, 738–747.
- Wetzel, R.G., 1995. Death, detritus and energy-flow in aquatic ecosystems. *Freshwater Biology* 33 (1), 83–89.
- Yoshiyama, K., Klausmeier, C.A., 2008. Optimal cell size for resource uptake in fluids: a new facet of resource competition. *The American Naturalist* 171 (1), 59–70.
- Zhao, J., Ramin, M., Cheng, V., Arhonditsis, G.B., 2008a. Competition patterns among phytoplankton functional groups: how useful are the complex mathematical models? *Acta Oecologica* 33, 324–344.
- Zhao, J., Ramin, M., Cheng, V., Arhonditsis, G.B., 2008b. Plankton community patterns across a trophic gradient: the role of zooplankton functional groups. *Ecological Modelling* 213, 417–436.



**EXAMINATION OF THE ROLE OF DETRITUS FOOD QUALITY,  
PHYTOPLANKTON INTRACELLULAR STORAGE CAPACITY, AND  
ZOOPLANKTON STOICHIOMETRY ON PLANKTONIC DYNAMICS  
(Electronic Supplementary Material)**

**Gurbir Perhar and George B. Arhonditsis\***

Ecological Modeling Laboratory  
Department of Physical and Environmental Sciences  
University of Toronto, Toronto, Ontario, M1C 1A4, Canada

\* Corresponding author

e-mail: [georgea@utsc.utoronto.ca](mailto:georgea@utsc.utoronto.ca), Tel.: +1 416 208 4858; Fax: +1 416 287 7279.

## FIGURES LEGENDS

**Figure SI-1.** Time series plots illustrating the shift from steady state equilibrium to oscillations along a hypolimnetic nutrient gradient. Zooplankton mortality and detritus food quality were set to moderate ( $d=0.25 \text{ day}^{-1}$ ) and low ( $FQ_2=0.2$ ) values, respectively. As the hypolimnetic nutrient concentration is systematically varied along a transect of relatively high illumination (dashed black line,  $b=0.05 \text{ m}^{-1}$ ) from Figure 1c, limit cycles emerge; (a)  $PO4_{(hypo)}=0.025 \text{ g P m}^{-3}$ , (b)  $PO4_{(hypo)}=0.05 \text{ g P m}^{-3}$ , (c)  $PO4_{(hypo)}=0.08 \text{ g P m}^{-3}$ , (d)  $PO4_{(hypo)}=0.15 \text{ g P m}^{-3}$ .

**Figure SI-2.** Time series plots illustrating the shift from steady state equilibrium to oscillations along a light availability gradient. Zooplankton mortality and detritus food quality were set to moderate ( $d=0.25 \text{ day}^{-1}$ ) and low ( $FQ_2=0.2$ ) values, respectively. As light availability is systematically varied along a transect of relatively high hypolimnetic concentration (dashed black line,  $PO4_{(hypo)}=0.10 \text{ g P m}^{-3}$ ) from Figure 1c, limit cycles degenerate; (a)  $b=0.01 \text{ m}^{-1}$ , (b)  $b=0.07 \text{ m}^{-1}$ , (c)  $b=0.14 \text{ m}^{-1}$ , and (d)  $b=0.20 \text{ m}^{-1}$ .

**Figure SI-3.** Parameter space exploration testing top-down vs. bottom-up control via regulation of the zooplankton mortality ( $d$ ) and nutrient availability ( $PO4_{(hypo)}$ ). The color map depicts phytoplankton biomass in panels *a,c,e* and phytoplankton to zooplankton ratio in panels *b,d,f*; the white contour delineates the oscillatory region(s). Light availability is set high ( $b=0.05 \text{ m}^{-1}$ ), while the detritus food quality is varied from low (panels *a & b*,  $FQ_2=0.2$ ), to intermediate (panels *c & d*,  $FQ_2=0.5$ ), to high (panels *e & f*,  $FQ_2=0.8$ ) values.

**Figure SI-4.** *(a)* Point attractor/steady state equilibrium trajectory; *(b)* Periodic attractor/limit cycle trajectory; *(c)* Global attractor; *(d)* Global repeller; *(e)* Saddle node; *(f)* Neutral saddle; *(g)* Bifurcation diagram depicting supercritical Hopf bifurcation; *(h)* subcritical Hopf bifurcation; and *(i)* Neimark-Sacker point shown in state space.



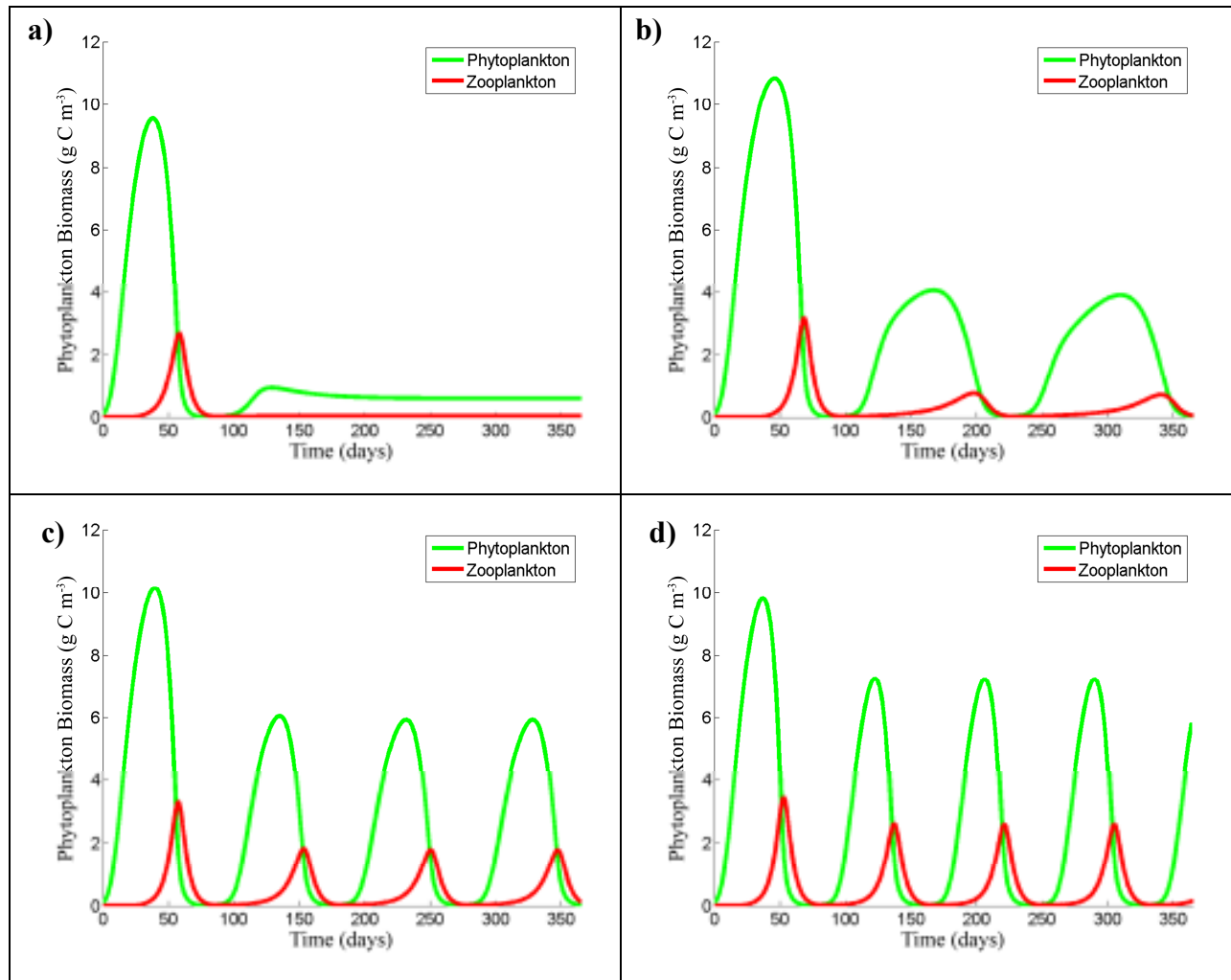


Figure SI-1

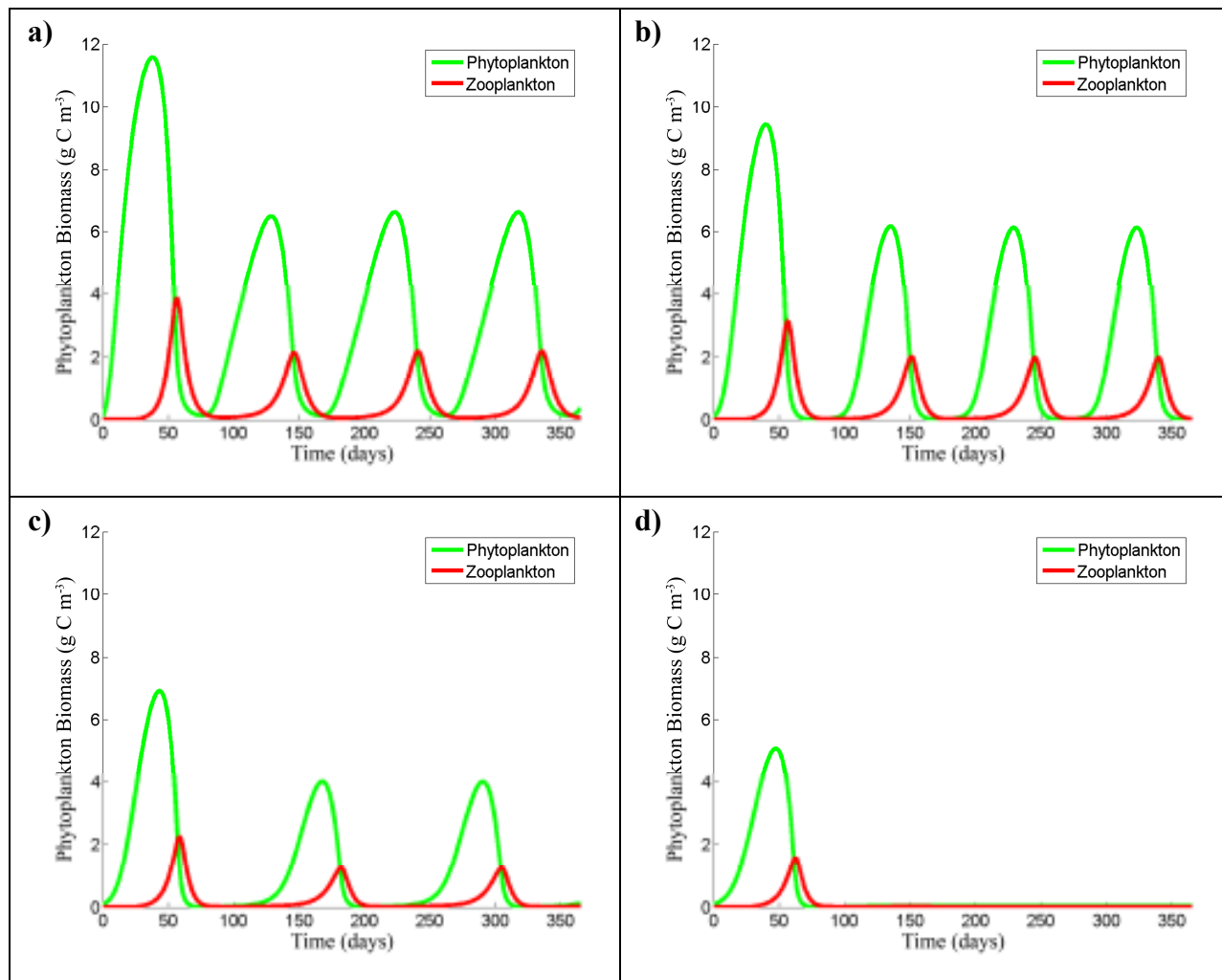


Figure SI-2

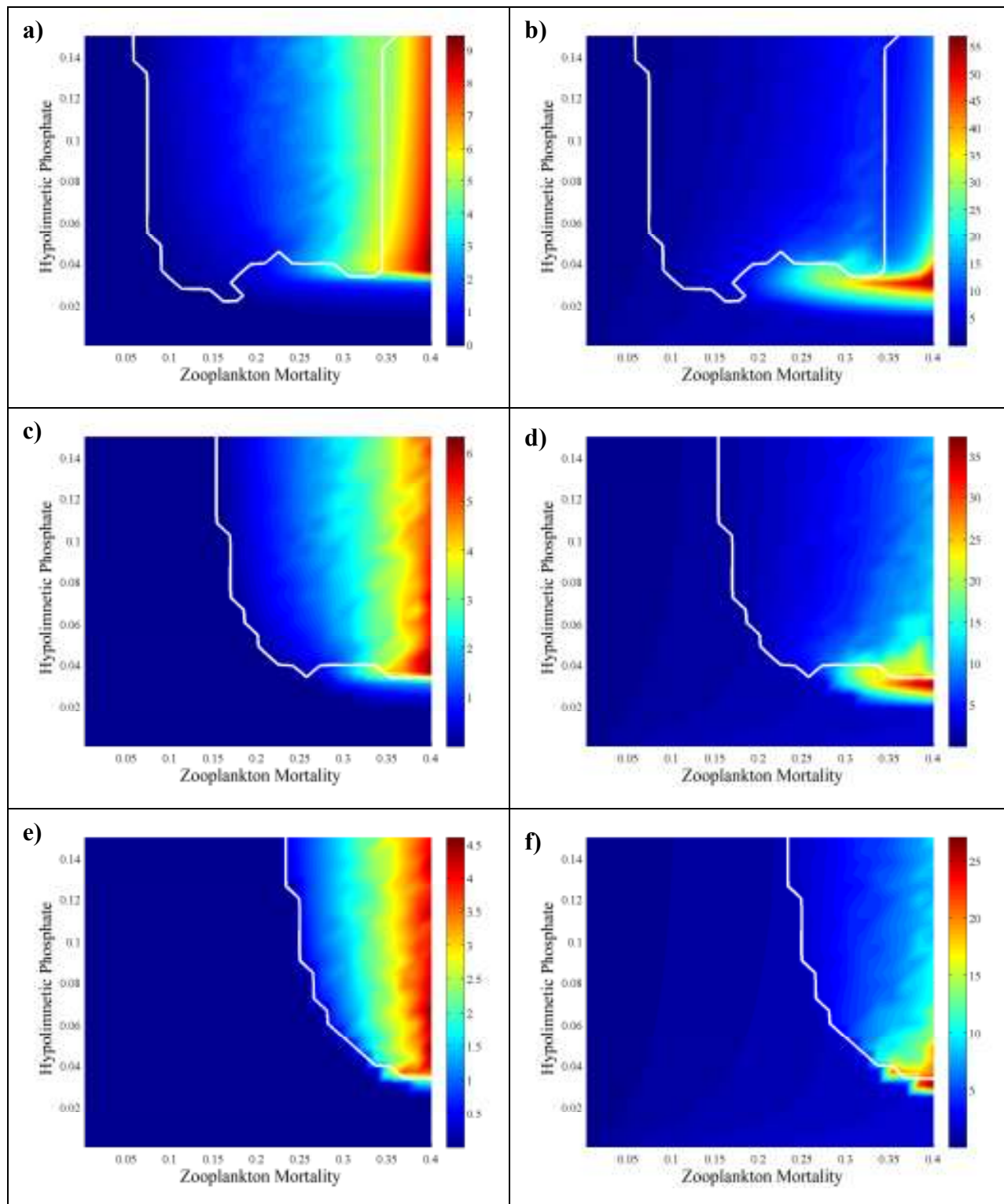
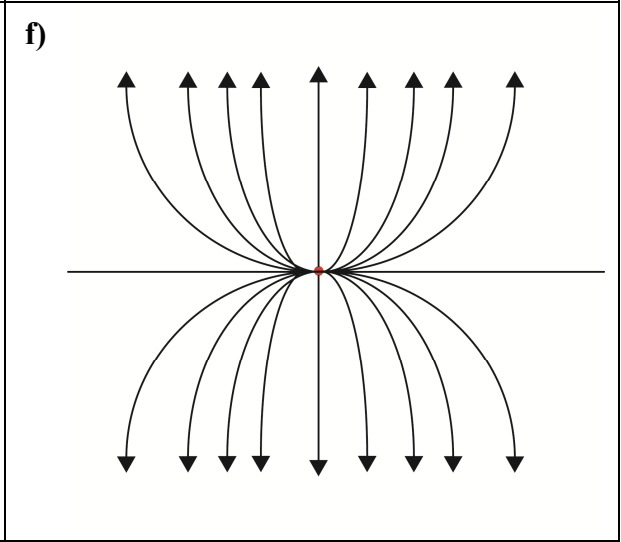
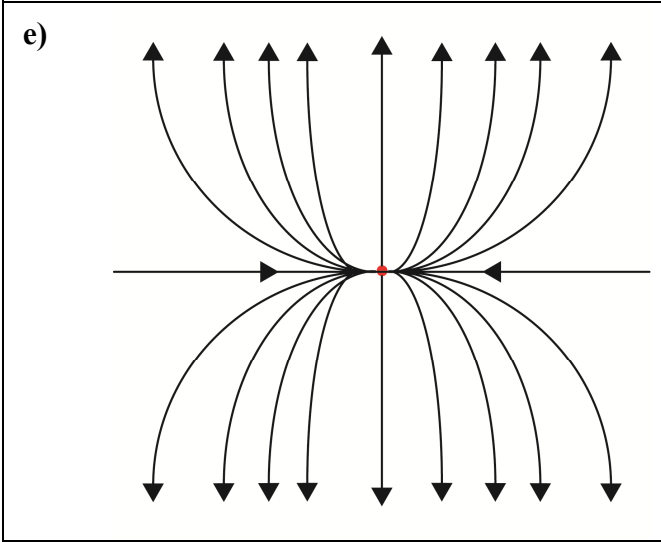
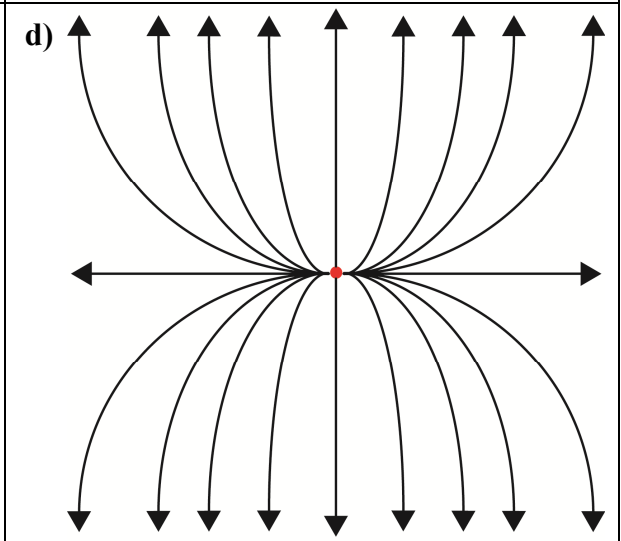
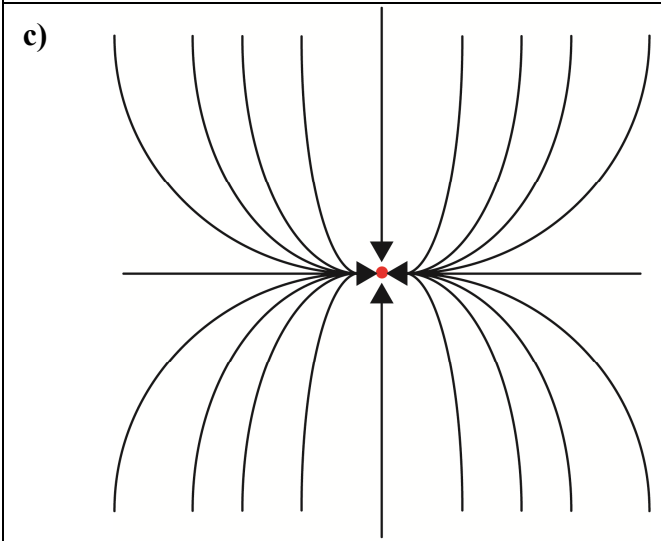
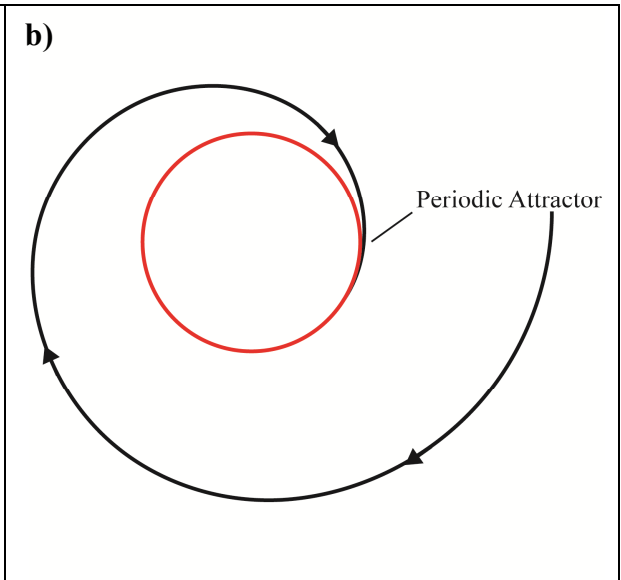
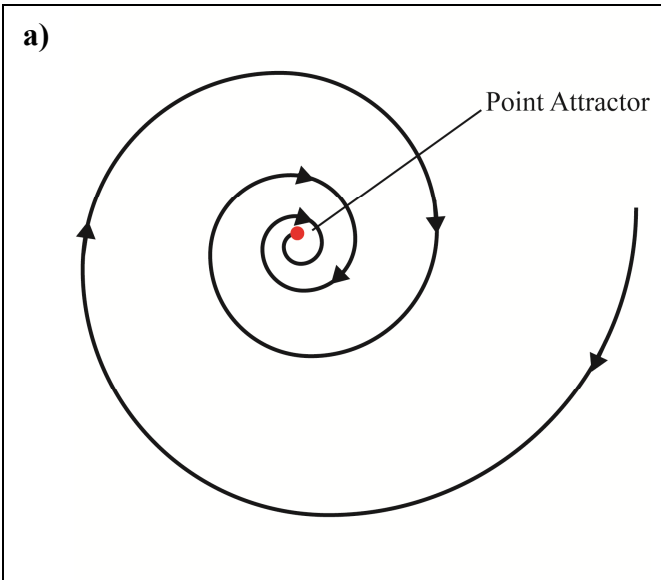
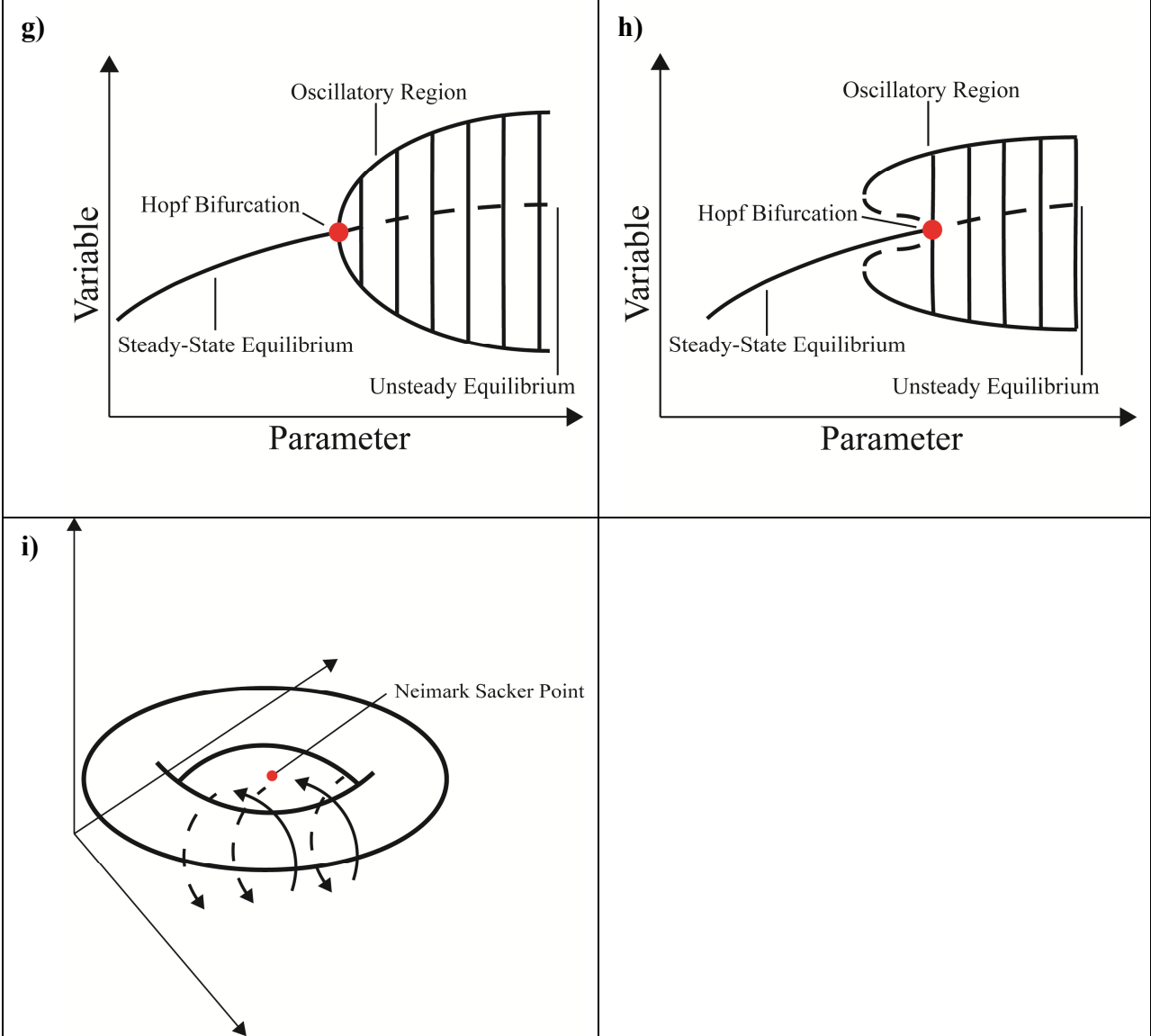


Figure SI-3







**Figure SI-4**